

NASA CONTRACTOR REPORT

NASA CR-2775



NASA CR-2775

0061362

TECH LIBRARY KAFB, NM

LOAN COPY: RETURN TO
AFWL TECHNICAL LIBRARY
KIRTLAND AFB, N. M.

ANALYTICAL STUDY OF ACOUSTO/OPTICAL HOLOGRAPHY - INTERFACING METHODS FOR ACOUSTICAL AND OPTICAL HOLOGRAPHY NDT RESEARCH

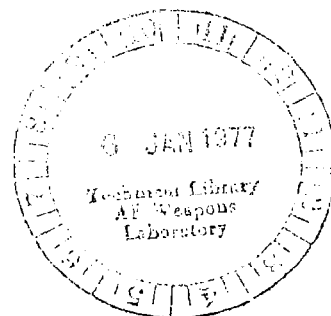
H. M. A. El-Sum

Prepared by

EL-SUM CONSULTANTS

Atherton, Calif. 94025

for George C. Marshall Space Flight Center



NATIONAL AERONAUTICS AND SPACE ADMINISTRATION • WASHINGTON, D. C. • DECEMBER 1976



0061362

1. REPORT NO. NASA CR-2775		2. GOVERNMENT ACCESSION NO.		3. RECIPIENT'S CATALOG NO.	
4. TITLE AND SUBTITLE Analytical Study of Acousto/Optical Holography — Interfacing Methods for Acoustical and Optical Holography NDT Research				5. REPORT DATE December 1976	
				6. PERFORMING ORGANIZATION CODE	
7. AUTHOR(S) H. M. A. El-Sum				8. PERFORMING ORGANIZATION REPORT # M-197	
9. PERFORMING ORGANIZATION NAME AND ADDRESS El-Sum Consultants 74 Middlefield Road Atherton, California 94025				10. WORK UNIT NO.	
				11. CONTRACT OR GRANT NO. NAS8-31783	
12. SPONSORING AGENCY NAME AND ADDRESS National Aeronautics and Space Administration Washington, D. C. 20546				13. TYPE OF REPORT & PERIOD COVERED Contractor	
				14. SPONSORING AGENCY CODE	
15. SUPPLEMENTARY NOTES Prepared under the technical monitorship of the Physics and Instrumentation Division, Space Sciences Laboratory, Marshall Space Flight Center					
16. ABSTRACT This report covers a study of the international status of the art of acousto-optical imaging techniques adaptable to nondestructive testing and, more important, to interfacing methods for acoustical and optical holography in nondestructive testing research. Evaluation of 20 different techniques encompassed investigation of varieties of detectors and detection schemes, all of which are described and summarized. Related investigation is reported in an Appendix. The report presents important remarks on image quality, factors to be considered in designing a particular system, and conclusions and recommendations for extension of this work. Three bibliographies are included. Compatible systems to be used with the MSFC hybrid system (optical, acoustical, and correlation) are a Bragg diffraction (direct optical-acoustical interaction) scheme and the electronically focussed and scanned piezoelectric array. Both systems have sensitivity approaching 10^{-9} to 10^{-11} W/cm ² and resolution approaching the acoustical wavelength in the tested material, are capable of real-time display, and can be designed for use in either a pure optical or an acousto-optical mode of operation. At the same time, a portable acoustic probe, akin to the probe used in medical diagnosis, can be designed for testing large objects on site.					
17. KEY WORDS			18. DISTRIBUTION STATEMENT Category 35		
19. SECURITY CLASSIF. (of this report) Unclassified		20. SECURITY CLASSIF. (of this page) Unclassified		21. NO. OF PAGES 96	
				22. PRICE \$4.75	

FOREWORD

This is the final reporting on a six man-month study of the state of the art of acousto-optical holography and its application in nondestructive testing (NDT). The project was funded by MSFC-NASA under contract NAS8-31783.

The goal of this project, in a broad sense, was to investigate the interfacing methods for acoustical and optical holography in NDT research in order to identify the acoustical holography schemes compatible for integration in a hybrid system utilizing other schemes (optical and correlation) for testing objects nondestructively, as envisioned by the MSFC Optics and Electro-Optics Branch (Figure 1). For completeness, the investigation encompassed a survey of various techniques of imaging, testing, and detection of flaws in materials with visual radiation, acoustics, x-rays, electrons, and infrared. However, only the nonholographic acousto-optical techniques which may compete favorably with the holographic schemes are included in this report. The in-depth study concentrated on the international state of the art of visualization of acoustic imaging, particularly with holography, and on evaluating the various techniques of transducing the acoustical information into optical information.

AUTHOR'S ACKNOWLEDGMENTS

Acknowledgment is due to many industrial, academic, and publishing organizations in the U. S. and Western and Eastern Europe for collecting information that aided in preparing this report. Communications with many researchers here and abroad, particularly with G. Wade, G. W. Stroke, R. L. Kurtz, M. G. Maginess, W. Anderson, B. Auld, and P. Greguss, have been quite valuable and gratifying.

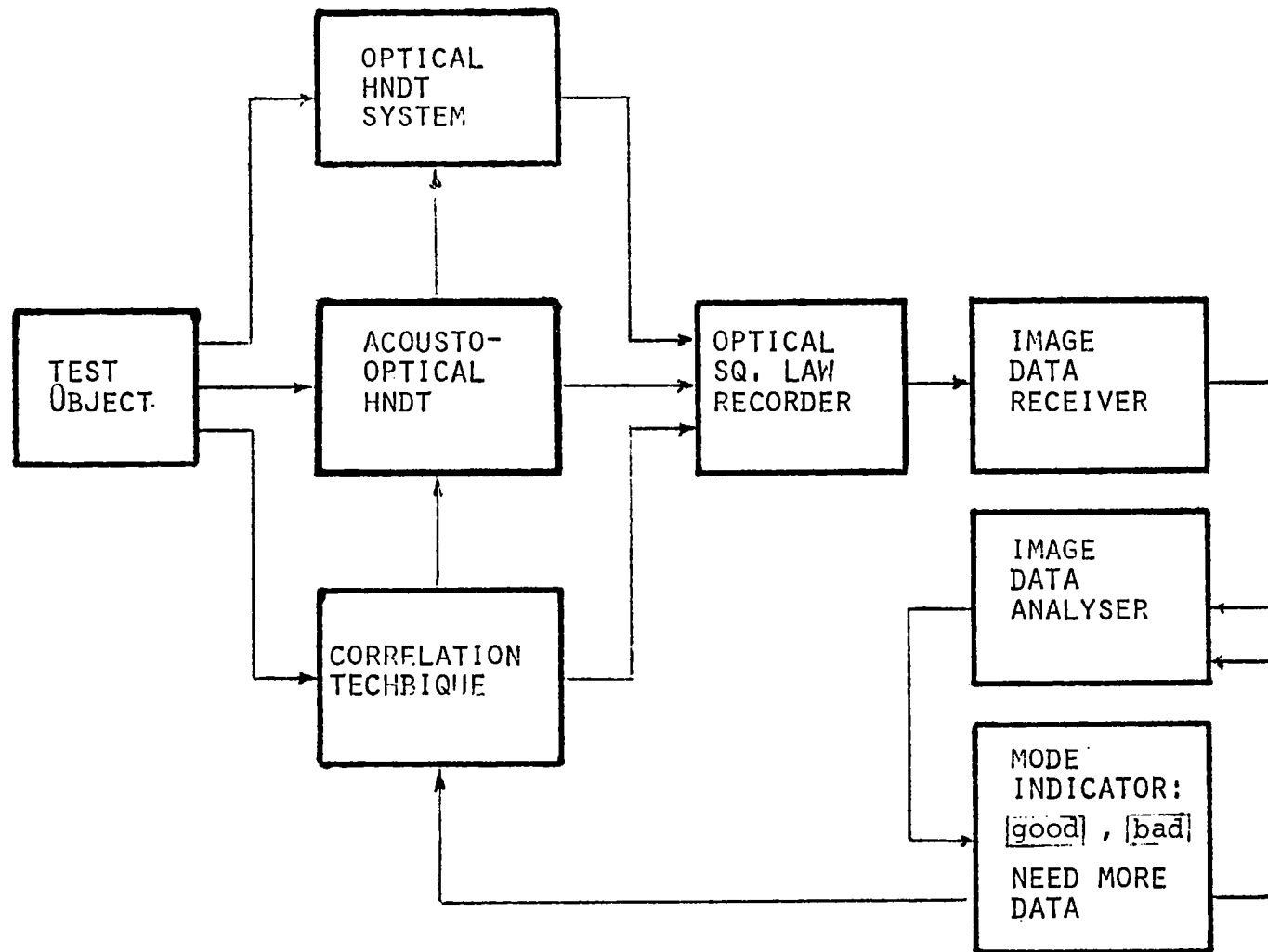


FIGURE 1. Flow chart of hybrid system for nondestructive testing, as conceived by MSFC-Optics and Electro-Optics branch.

TABLE OF CONTENTS

Page

CHAPTER I

GENERAL INTRODUCTION	1
----------------------	---

CHAPTER II

ACOUSTICAL IMAGING SYSTEMS	5
----------------------------	---

2.1	Introduction	6
2.2	Liquid Surface Deformation (Static Ripples)	8
2.3	Bragg Diffraction or Direct Sound-Light Interaction	10
2.4	Laser Beam Scanning	16
2.5	Electron Beam Scanning of Deformed Surface	16
2.6	Sokolov Image Tube Converter	18
2.7	Metal Fiber Face Tube Image Converter	20
2.8	Pyroelectric Image Converter and Image Storage	21
2.9	Electrostatic Transducer	22
2.10	Piezoelectric Array With Electronic Focussing and Scanning	23
2.11	Frequency Swept Holographic Imaging	26
2.12	Zone-Plate Acoustic Imaging Devices	27
2.13	Gabor's Sonaradiographic Imaging Scheme	30
2.14	Acoustic Tomography	33
2.15	Piezoresistive Image Converter	33
2.16	Electroluminescent Acoustic-Image Detector	34
2.17	Photographic and Chemical Direct Acoustic Recording	34
2.18	Solid and Liquid Crystal Acoustic Displays	40
2.18.1	Dynamic Scattering	41
2.18.2	Voltage Controlled Optical Activity	42
2.18.3	Guest-host Interaction	42

TABLE OF CONTENTS (Cont'd)

	<u>Page</u>
2.18.4 Birefringent Properties	43
2.18.5 Direct Acousto-Optical Effects	43
2.19 Pohlman Cell	44
2.20 Oil, Thermoplastic and Photoplastic Films	44
2.21 Scanning and Sampling Technique	46
2.22 Recent Developments	47

CHAPTER III

ANALYSIS, CONCLUSIONS AND RECOMMENDATIONS

3.1 Image Quality	50
3.2 Comparison of Various Techniques	52
3.3 Recommendations	53
 BIBLIOGRAPHY	 60
 APPENDIX A - Earlier Study of the Project	 A-1
 APPENDIX B - Real-Time, Erasable Image Recording	 B-1

LIST OF FIGURES

<u>Number</u>		<u>Page</u>
1.	Flow chart of hybrid system for nondestructive testing as conceived by MSFC-Optics and Electro-Optics Branch	vii
2.	Liquid surface deformation (static ripples) system . .	9
3.	Bragg diffraction acoustical imaging system	11
4.	Pulse Bragg diffraction system for NDT in air	13
5.	Laser beam scanning	17
6.	Sokolov tube image converter	19
7.	Piezoelectric array electronic focussing and ASW scanning	25
8.	Zone plate acoustic imaging - operating arrangement . .	28
9.	Fabrication of zone-plate transducers	29
10.	Light projected zone-plate acoustic transducer	31
11.	Piezoelectric electroluminescent acoustic image detector	35
B-1	Operation of Ruticon image devices	B-4
B-2	Read-out of Ruticon device	B-5

LIST OF TABLES

<u>Number</u>		<u>Page</u>
I.	Acoustical imaging methods and detection	55
A-I	Ultrasonic detectors	A-6
A-II	Frequency range for different applications	A-6

CHAPTER I

GENERAL INTRODUCTION

The potential of acoustical holography as a diagnostic tool in nondestructive testing was well recognized ever since the first successful demonstration of forming an acoustical hologram and reconstructing it with coherent visible light.^(1,2) In fact, the vigorous development of acousto/optical holographic techniques for material nondestructive testing is second only to the application of these techniques in the biological and medical field, as evidenced from the yearly symposia on Acoustical Holography,⁽³⁾ the IEEE ultrasonics,⁽⁴⁾ and other national and international conferences. Technological advances, inspired originally by acoustical holography, have led in many cases to further simplification of the two-stage acoustical holography to a real-time acoustical imaging, as will be discussed later.

Among the pertinent advantages of acoustical holography in NDT are:

- (1) having a permanent 2-D record of a 3-D image (both outer shape and internal structure of the object),
- (2) obtaining a good lateral resolution without the need for complex ultrasonic imaging optics,
- (3) obtaining a good depth resolution without the need for very short pulses of ultrasonic energy,
- (4) detection of very weak ultrasonic scattering regions, too weak to be detected by other methods,
- (5) measuring the degree of material uniformity by considering the hologram as an interferogram,
- (6) measuring the uniformity of the tested object before and after a change in its environment (such as temperature, pressure, etc.), and

- (7) converting the acoustical information into optical information which may be easier to interpret directly by the eye or by the use of well established optical techniques.

However, acousto/optical imaging capabilities have certain limitations and what may be considered disadvantages. As an illustration, the following examples are enumerated:

- (1) distortion due to the change in wavelength (from a long acoustical wave λ_s which probes the object and forms the hologram, to a much shorter light wave λ_L to reconstruct a visible image). See the discussion in Appendix I, pp. A-4.
- (2) the speckle effect produced by the coherent nature of the reconstructing light, and the limited aperture of the hologram.
- (3) at certain angles of incidence, objects, opaque to sound waves, become transparent to such waves and hence the introduction of possible misinterpretation of the image.
- (4) nonlinearity of sound propagation introduces distortion in the phase of the reflected waves, particularly with high amplitude and frequency.
- (5) acoustic transducers usually have an excess of 100 dB (a factor of 100,000) range of pressure amplitudes, while the intensity modulated oscilloscope can only display about 20 dB (a factor 10), and photographic films have a dynamic range of only about 10 dB.⁽¹⁰⁹⁾ Thus to display both large and small acoustic information simultaneously, it is necessary to use amplitude compression technique or use digitizing

techniques and computer processing.

- (6) distortion due to mechanical instability of tested object or to unsteady environment, in which case special mounting⁽⁵⁾ may be needed.

Most of these limitations can be overcome. They are mentioned merely to emphasize the need for extreme care to correctly diagnose the tested object using the acousto/optic holographic technique. Furthermore, it shows the necessity of using the acousto/optical testing as a complement to other testing means such as optical, and correlation.

Acoustic frequencies ranging from 100 KHz to 10 GHz have been used in NDT [see Appendix A, pp. A-6, Table A-II]; the choice of the proper frequency depends upon the material of the object to be used, and the required depth of penetration of the probing wave, since the attenuation of such wave is proportional to the square power of the frequency. Hence usually the normal NDT of thick objects are limited to the acoustic frequency range of 100 KHz to 10 MHz, while the range 10 MHz to 10 GHz is used in ultrasonic microscopy where the material is quite thin (of the order of micrometers). The latter will not be treated extensively in this report; however, this does not diminish its importance in areas like the study of the theory of crack development in materials. New materials and/or techniques (e.g., photopolymer films, pyroelectric conversion layers, electrostatic transducers, crystalline solid thin layer of $\text{CoCl}_2 \cdot 6 \text{H}_2\text{O}$, ultrasonic tomography, zone plate focussing, electronic focussing and scanning of phased arrays) still in the developing state, are described in Chapter II, and evaluated in Chapter III.

CHAPTER II

ACOUSTICAL IMAGING SYSTEMS

2.1 Introduction

An acoustical imaging system consists, in general, of:

- an insonifier
- the object
- a lens (not needed in some systems)
- a detector or transducer
- a display or recorder (which may be the detector itself).

All of these components are usually immersed in a water tank to minimize the acoustical impedance mismatch.* Some of these components may be a simple one element, a composite structure, or a collection of several elements, depending on the operational function of the whole system.

There may be, for example, more than one insonifier, as in holography; the lens may be eliminated in some holographic arrangements, or if the object is in contact with the detector; the detector itself may be (but rarely in a practical system) a simple chemical emulsion, a liquid crystal, a composite of deformed liquid or solid surface and a scanning laser or electron beam, a sandwich of several materials (e.g., piezo-electric and electroluminescence) etc.; the visual display of the acoustical information is converted into optical information via a vidicon camera, an optical telescope, or a CRT. There is quite an overlap between the display subsystem and the detection techniques that it is often difficult to separate the two.

* Acoustical imaging reveals the change in acoustical impedance in the object, and hence depends on the density of the material to be imaged and the acoustic velocity within this material. This is different from x-ray imaging which depends on the electron density and atomic number of the material; electron beam images (as in electron microscope) reveals only the surface or near surface structure, and depends on the atomic density of the material; optical images reveal only the outer shape of the object.

The different components of an acousto/optical system are arranged in a variety of ways, depending on whether the object is to be seen in a transmission or a reflection mode. In the transmission mode the object hides the detector from the insonifying source. If the object is in touch with the detector, the lens is not needed and we get an arrangement akin to a contact print in optical or x-ray photography. However, if the object is separated from the detector then a lens is needed between the two to cast a sharp image on the detector; otherwise, if there is no lens, the shadow cast on the detector may be a diffused shadow, or an on-axis (Gabor type) hologram.* An off-axis acoustic hologram may be formed if the shadow of the object cast on the detector is biased by another coherent acoustic wave (from another insonifier tuned to the same frequency) which falls obliquely on the same detector. In the reflection mode arrangement, the object, insonifier and detector, are not in a straight line. The scattered wave from the object may be focussed on the detector by a lens; or, in the absence of a lens, an off-axis hologram is produced. Here again, a second reference acoustic wave may be used, particularly if an in-focus hologram is to be made.

In an earlier study (summarized in Appendix A) we broadly classified the various systems, mainly according to the detection-display scheme. Now, we shall proceed to expound the various techniques, concentrating mainly on those most applicable to NDT.

* Such a hologram is produced only if acoustic radiation from the same source falls on the detector (without passing through the object) to provide the reference wave. It is assumed that coherent acoustic waves are used to insonify the object.

2.2 Liquid Surface Deformation (Static Ripples)⁽²⁷⁾

This method of acoustic image conversion and the electron-beam scanning tube of Sokolov are the earliest to be conceived for real-time visualization of ultrasonic images.^(11,12) When an acoustic image is focussed onto the liquid surface it causes the surface to elevate at each point until equilibrium is attained by the restoring forces of surface tension and gravity. The relief pattern formed in this way is an analog of the pattern of acoustic intensity incident on the surface. The deformed fluid surface serves as an optical phase-object, and a visible representation of the acoustic image is produced by reflecting light from, or refracting it through, the surface, using one of several phase-contrast imaging techniques. This technique has recently been revived in acoustic holography.^(1,2,12,13) The modern version (used commercially) is illustrated in Figure 2, which is self-explanatory. Refer to Appendix A, pp. A-7 - A-10 for more discussion.

Instead of the coherent acoustical reference beam, Green⁽¹⁵⁾ used a wire grating close to the liquid surface on which the acoustic image of the object is immersed. In this way the undesired high frequency ripples are reduced considerably. Both arrangements produced images of comparable quality.

Another improvement was made by N. K. Sheridan,⁽¹⁴⁾ to amplify the ripples, more at the high frequency end than the low frequency one, and hence reduce the low frequency noise and improve the real-time image visualization. He used a thin layer of a dielectric liquid (which may have conducting or insulating surface) placed in a strong electric field. Experimental verification of the idea revealed pictures no better than

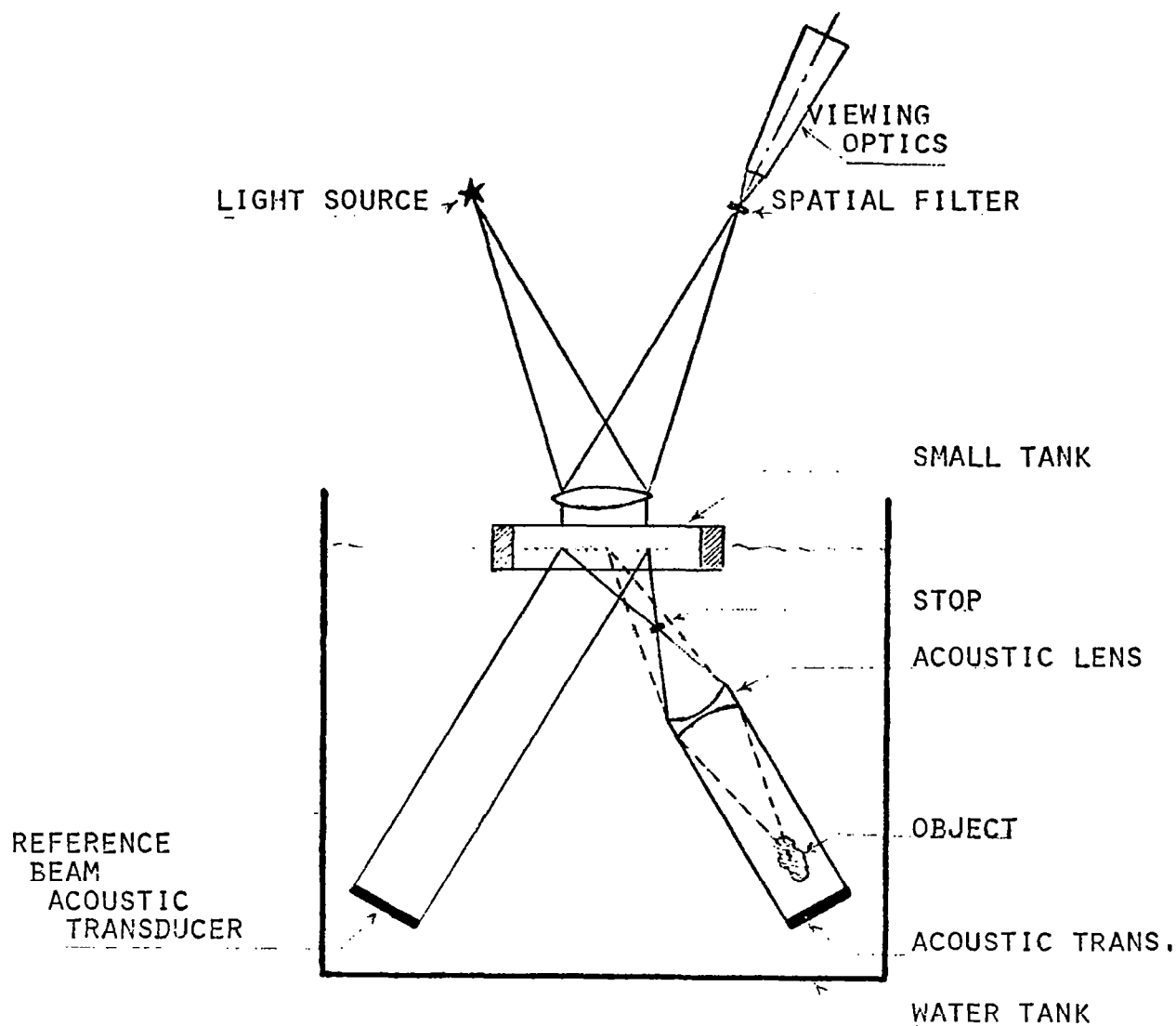


Figure 2. Schematic diagram of the basic arrangement for in-focus, real-time holography with the liquid surface deformation method. The object and reference insonifiers are immersed in a large water tank. A sharp image of the object is projected on the surface of the small tank (containing a low surface tension liquid), and is biased by the coherent reference wave to form an in-focus hologram in the form of ripples on the surface. Incident from above is a light beam from an unfiltered super pressure mercury vapour source. Its diffracted components are filtered and viewed in real-time by the viewing optics.

Brenden's and Green's, but the sensitivity may have been increased. This work has been discontinued.

The advantages of this technique are its

- (a) simplicity
- (b) moderate sensitivity (0.0015 W/cm^2 is practical; 10^{-9} W/cm^2 highly theoretical⁽¹⁷⁾)
- (c) good resolution (0.07" voids in 4" thick steel and 0.03" voids in 1" Al have been reported)⁽¹⁶⁾
- (d) capacity for real-time display

On the other hand, this scheme is most suited for Gabor-type, near on-axis holography because of the limited frequency response of the liquid surface. Depending on the surface tension of the liquid the low and high spatial frequency cut-offs are at about 1 cycle/cm and 20 cycle/cm respectively. Furthermore, the highest acoustic frequency that can be used is about 10 MHz (limited by the surface tension of the liquid) and the lowest usable acoustic frequency is about 0.5 MHz (limited by the capillary forces giving way to gravitational forces).

2.3 Bragg Diffraction or Direct Sound-Light Interaction⁽¹⁸⁾

The operational principle of Bragg-diffraction imaging is based upon the diffraction of coherent light by acoustic waves when proper conditions are met. A basic schematic arrangement of the system is shown in Figure 3. The object is placed on a membrane in the water filled Bragg acoustic cell, and insonified in the vertical direction. The laser beam interacts with the acoustic wave propagating in the acoustic cell. Two spherical lenses collimate the laser beam, which is then focussed by a cylindrical lens onto the line P_1 . Bragg diffraction

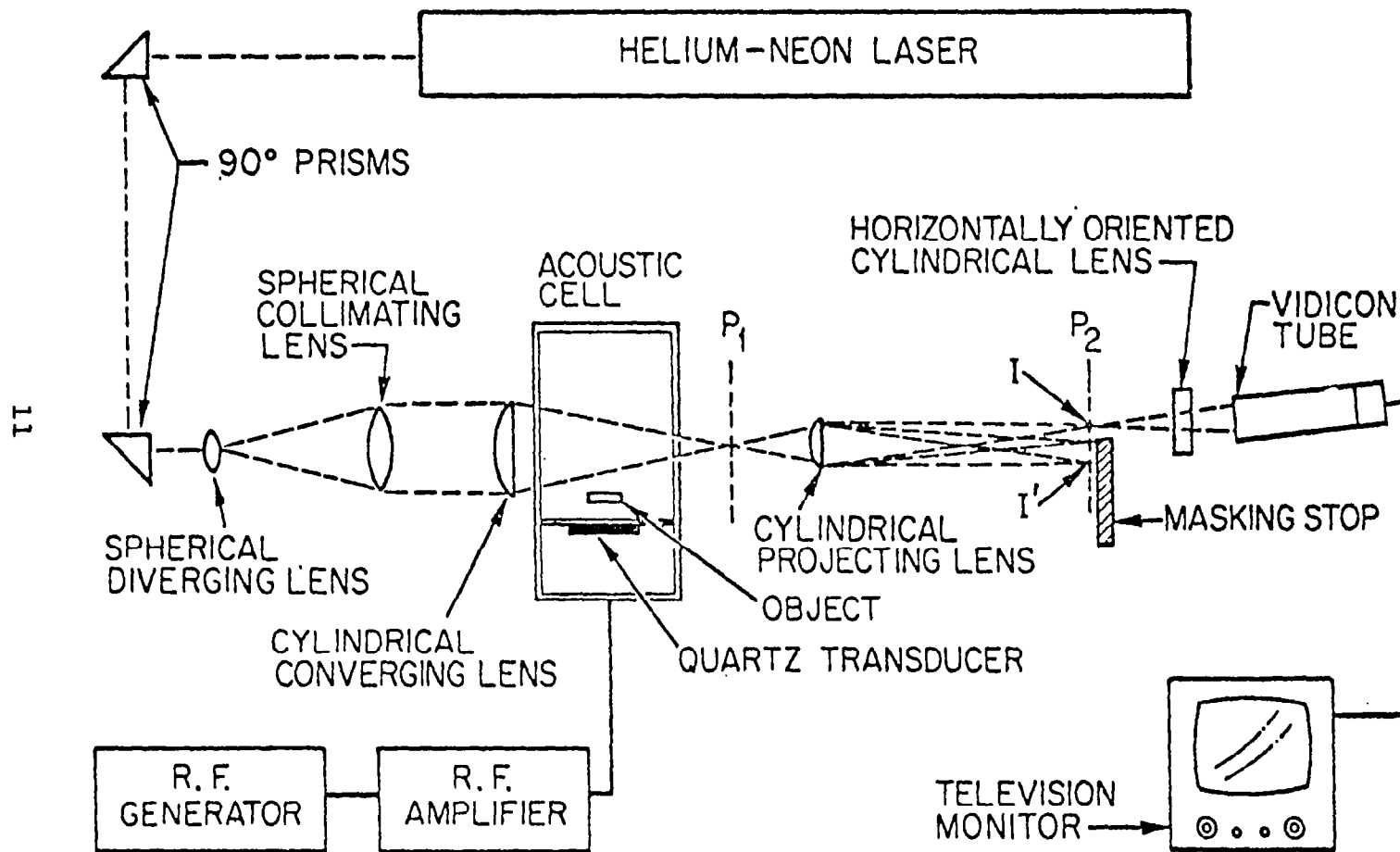


Figure 3. Schematic diagram of Bragg diffraction acoustical imaging system. Coherent light from the laser interacts with the acoustic wave in the Bragg acoustic cell. The light and acoustic waves are propagating perpendicular to one another. Visible image is displayed on the TV monitor.

of the light takes place in the acoustic cell. Two first-order frequency shifted Bragg-diffracted light beams, I and I', and the zero-order light at its original frequency, are projected onto plane P_2 . Only one of the diffracted beams is allowed through a second cylindrical lens for aspect ratio correction and is projected onto a vidicon tube for real-time television display.

The angle of diffraction in this scheme is a function of the ratio of the light wavelength to the acoustic wavelength, according to the simple equation:

$$\sin \theta = \frac{\lambda_L}{2\lambda_s} \quad (1)$$

where θ is half the angle of diffraction. It is therefore desirable to use the highest possible acoustic frequency. Frequencies in the range of 10 to 100 MHz have been used. At the lower frequencies, the produced images always suffer from the scattering of the direct beam. To overcome this, an ingenious scheme was used, where the image is recorded with a biasing light wave from the laser. This recording will then carry the desired image superimposed on a hologram of the direct beam (since the diffracted light has a different frequency from the original laser light). The recording can then be reconstructed in the normal way and the desired image can be filtered out.

This technique demonstrated its usefulness in NDT. However, it needs the immersion of the object in water. To eliminate this in order to test objects in air, R. A. Smith devised the arrangement shown in Figure 4. Electric energy which generates the sound is also sent to a delay line that feeds an electronic shutter controlling the emission

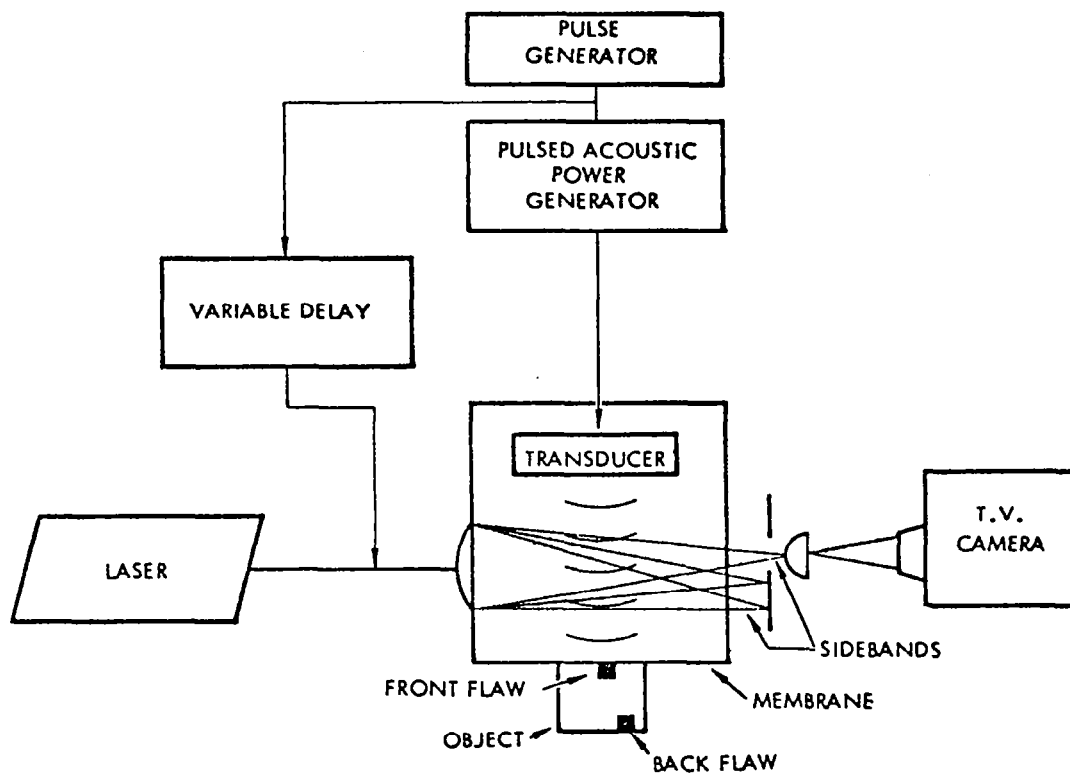


Figure 4. Block diagram of pulsed Bragg imaging system for NDT of material that must be kept dry (i.e. not to be immersed in the water filled Bragg cell). The object is placed in air against the polyethylene membrane of the Bragg cell. The pulsed light from the laser is delayed so that it passes through Bragg cell only when the acoustic pulse is reflected upwards from the object. The delay time determines the plane of the object to be imaged, and the thickness of such a plane is determined by the duration of the laser light pulse.

of laser light. By pulsing the laser at some given time, subsequent to the generation of sound, reflected sound will be returned from a specific distance within the object viewed. At a later time, the sound present in the Bragg cell would be reflected from a greater distance in the object. Consequently, the image will be a replica of objects located at ever increasing distances as time proceeds. The duration of the laser light pulse is made sufficiently short to have a negligible effect on the size of the range interval viewed. The range interval is one-half the duration of the sound pulse multiplied by the velocity of sound in the material inspected. Flaws outside this range interval will be rejected from view. Flaws may be separated which are as close together as pulse rise or fall times will allow. A complete inspection of an object would require repetitive pulsing of a sound transducer with repetitive illumination from the laser using sound pulses and laser pulses which are repeated with increasing delay after a given image plane has been inspected. Pictures have been published⁽²³⁾ using this technique with an acoustic frequency of 18.7 MHz, of holes in Al block, silicon rubber strips on Al, etc.

The resolution in this arrangement depends on the acoustic wavelength λ_s , the distance of interaction D in the Bragg cell, the angular extent 2α of the converging light, the distance R between the object and light column, the height H of the light column in the vertical direction, and the width W of the light cone. The horizontal and vertical resolutions, δ_h and δ_v respectively, are different:

$$\delta_h = \left\{ \begin{array}{ll} R \frac{\lambda_s}{D} & \text{for } R > \frac{D}{2 \sin \alpha} \\ \frac{\lambda_s}{2 \sin \alpha} & \text{for } R < \frac{D}{2 \sin \alpha} \end{array} \right\} \quad (2)$$

$$\delta_v = \left\{ \begin{array}{ll} R \frac{\lambda_s}{H} & \text{for } R = H \\ \Lambda & \text{for } R \ll H \end{array} \right\} \quad (3)$$

The maximum number of resolution cells occurs when the object is adjacent to the light column. In this case the number of these cells in the vertical direction is equal to H (expressed in terms of λ_s).

In the horizontal direction, the number of resolution cells is

$$N_h < \frac{W}{\lambda_s} \quad (4)$$

Thus for $\lambda_s = 0.075 \text{ mm}$, $W = 25 \text{ mm}$ and $H = 100 \text{ mm}$, N_h is less than 333.

The advantage of the Bragg Diffraction scheme are:

- (1) Extreme simplicity
- (2) Sensitivity (comparable to the surface deformation technique)
- (3) High resolution (due to the use of high acoustic frequencies and which may approach λ_s in an idealized system; $3 \lambda_s$ has been reported⁽²²⁾).
- (4) Capacity for real-time display.

On the other hand, the field of view is rather limited and although the system can be used for NDT, it is most suited for microscopy.

2.4 Laser Beam Scanning^(24,25,26,28,100,101)

In this technique a scanning laser beam is used to effect optical readout of the acoustic information which is present in the form of dynamic ripples on solids or liquids. It is mostly limited to acoustic microscopy because it has an extremely limited aperture, due to the limitation of the angular deflection of the laser beam. It has not been used except for imaging very thin samples, mostly biological, using acoustic frequencies near 100 MHz. Interested readers are referred to the literature referenced above, and to Appendix A, pp. 11.

It has demonstrated its real-time operation capability using 100 MHz, displaying simultaneously the acoustic and optic images of the tested samples (25 μm thick) in an arrangement shown in Figure 5. The measured sensitivity of this technique is 10^{-3} W/cm^2 , while theoretically it should reach about 10^{-9} W/cm^2 .

It has recently been reported, however, that displacements were measured of the order of magnitude of 0.07 \AA over 15 cm aperture with acoustic frequency of 10 MHz.⁽²⁹⁾ Argon laser was used for scanning, using a moving mirror to study biological tissues, 6 μm thick, and also to measure the radiation pattern of acoustic transducers. This system sensitivity was 10^{-11} W/cm^2 .

2.5 Electron Beam Scanning of Deformed Surface⁽³⁰⁾

Instead of the laser beam scanning, discussed in the previous section, electron beams can be modulated in phase when they scan a photocathode on which the acoustic object-wave (focussed, unfocussed, or biased by a reference wave) is projected. This scheme is thus capable of displaying either a hologram or its optical reconstruction, depending

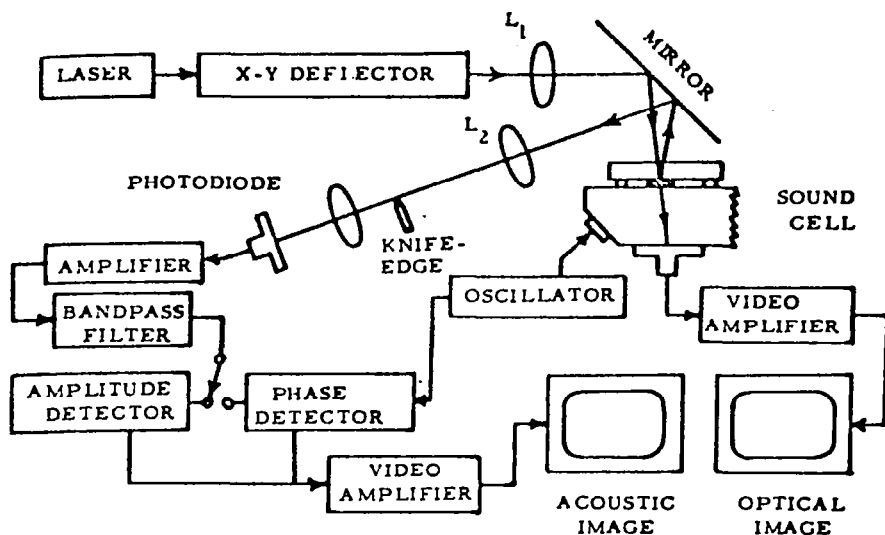


Figure 5. Laser beam scanning arrangement. The laser beam, reflected from the mirror, scans the acoustic field (in the sound cell) to be visualized. The exit pupil of the deflector is focused on the knife edge, and hence the position of the light beam remains independent of the instantaneous scan angle and depends only upon the surface distortion in the sound cell. The motion of the mirror causes the light intensity to be modulated (since the knife edge is arranged to block half the light beam). This intensity modulated light is collected by a photodiode and the resulting electrical signal, which is coherent with the local sound pressure, is amplified, filtered, detected, and fed into a TV monitor. The system is also capable of producing an optical image of the specimen (in the sound cell) and display it on an adjacent TV monitor.

on the relative location of the photocathode in the system .

2.6 Sokolov Image Tube Converter^(31,32,37,38,63)

This is one of the earliest acousto/optical image converters. Such a tube is shown as part (11) of Figure 6. It consists of a transducer (5) (a piezoelectric crystal) on which the acoustic image is projected, creating an electric potential pattern of that image. An electron beam scans the crystal and produces modulated secondary emission which records the image either directly on a photographic film, or projects it on the face of a CRT or a TV monitor. The arrangement shown in Figure 6 is capable of displaying a direct image of the object, its on-axis hologram or off-axis hologram which may be reconstructed later with coherent laser light in the normal fashion. It has also been used to form holograms with simulated electronic reference beam (32,33,34) and temporal holograms.^(35,36)

The advantage of this technique lies in both the high sensitivity (10^{-9} W/cm²) of the detected signal and the speed of scanning (30 frames per second). On the other hand, it has a limited angular field of view (5 to 15 degrees from the perpendicular to the transducer) and limited resolution. For higher resolution, the transducer should be as thin as possible, but the thinner it is, the weaker it will be mechanically and hence the smaller will be the aperture. Moreover, the transducer should operate at its resonance frequency, which means that the transducer thickness should be of the order of half the acoustic wavelength. All these parameters are related according to the equation of the minimum resolvable distance

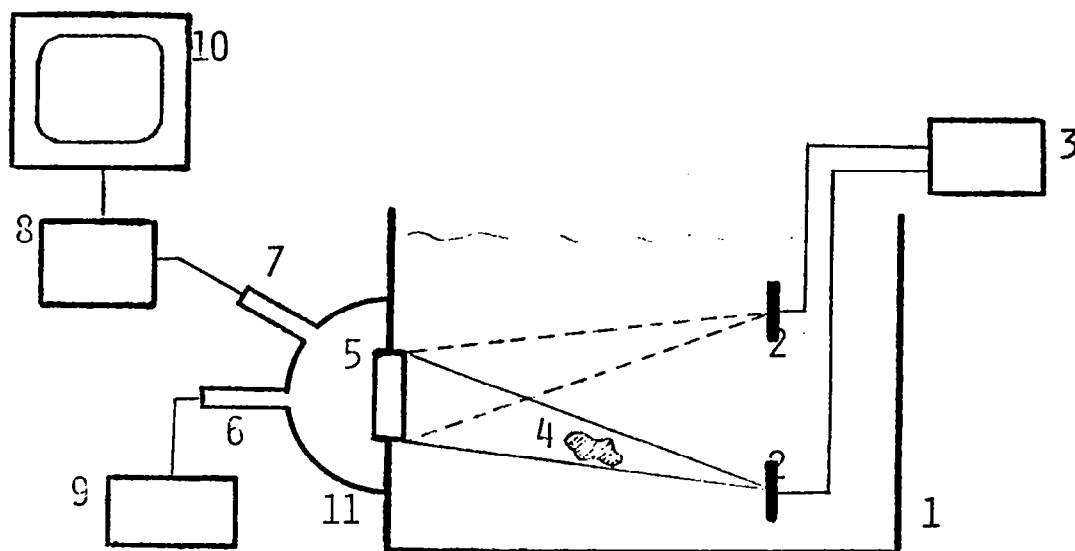


Figure 6. Sokolov image tube set up for acousto-optical imaging. Immersed in the water tank (1) are two acoustic transducers (2) fed by electronic generator (3). Acoustic beams from the transducers (2) impinge upon quartz (5) which is the face of the image tube (11). One of the beams is scattered by the object (4) and the other is the reference beam. Thus an acoustic hologram is formed on (5) in the form of an electric potential pattern across (5). The electron gun (6) scans (5), inducing secondary emission which is multiplied by the electron multiplier (7), amplified by (8) and finally displayed on a TV monitor (10). Block (9) represents the electronic circuits for electron beam generation and deflection.

$$\delta(\text{mm}) = \frac{2.86}{\text{Acoustic frequency (MHz)}} \quad (5)$$

Resolutions of 3 to 5 times the acoustic wavelength have been reported⁽³⁹⁾. Again, because of the mechanical rigidity, frequencies higher than about 10 MHz are not used. The interest in improving this image converter (because of its sensitivity and real-time capability) is continuing. All the efforts are concentrated on developing larger and thinner face plates. These special designs^(37,38) extend the common quartz face plate's diameter from 5 cm, used with 1 MHz, to 11.5 cm, used with 2 MHz, and even to 30 cm, used with 20 MHz. These results were attained by mechanically strengthening the piezoelectric quartz face plate⁽³⁷⁾ by a metal grid and/or modifying the electronic scanning scheme of the face plate.

Other types of face plates are discussed below.

2.7 Metal Fiber Face Tube Image Converter⁽⁴⁰⁾

The conventional Sokolov tube described above utilizes a piezoelectric plate (PZT-4 or quartz) to convert the incident acoustic signal into an electric signal, and also to serve as the interface between the vacuum chamber and the water. The plate should be as thin as possible, and for maximum resolution, the acoustic velocity in the plate should be about the same as that of the water so that the maximum angle of incidence for acoustic plane waves will be as close to 90° as possible. This puts severe limitation on the diameter of the face plate and the angular field of view. To overcome these limitations, a metal fiber face plate is used to serve as the interface between the vacuum chamber (piezoelectric plate) and the water. This metal fiber face plate is

made of glass clad wires (about 0.05 mm in diameter on about 0.15 mm centers). Theoretically there is no limit on the size of such a plate and in practice, 150 mm diameter plates were made. The limit is partially imposed by the angular deflection of the electronic scanner.

Published results indicate that such image converters increase the field of view of the Sokolov tube, does not degrade the resolution, and makes it possible to have a mechanically strong vacuum boundary while still being free to select an acoustic to electric transducer that will provide optimum image quality.

Instead of the metal fiber plate discussed above, one may be able to improve the characteristic acoustic impedance coupling between the water and the piezoelectric (quartz) plate by using fine copper powder in a casting plastic. The thickness of this material deposited on the quartz plate must be an odd number of quarter wavelength resonant point. Such a face plate has low absorption of the incident energy; however, it produces loss of resolution⁽³⁸⁾, due to the increase in thickness of the face plate.

2.8 Pyroelectric Image Converter and Image Storage⁽⁴¹⁾

The scanning beam interaction with the piezoelectric face of the Sokolov tube is such that only the energy in the piezoelectric element during the time interval the scanning beam is touching that element is effective in forming the visual signal. This characteristic operation has precluded for all practical purposes the use of pulsed acoustic radiation in systems using Sokolov tube.

To overcome this difficulty and further improvement (such as eliminating the high frequency cut-off limit, increasing the bandwidth,

increasing the sensitivity with the applied frequency, etc.) the piezo-electric face plate was replaced by an acoustic sensitive pyroelectric target which provides image storage in the form of a spatial temperature differential related to the absorbed acoustic energy. Only recently have such highly sensitive pyroelectric materials become available.⁽⁴²⁾ Thus pulsed acoustic radiation can be used and the image can be stored in the form of a thermal distribution in the pyroelectric layer. The pyroelectric material used is a crystalline substance, triglycine sulphate. It is spread as a layer of pyroelectric polymer (PVF₂) on pyrex glass. Such a detector is thermovoltaic, and has a spontaneous polarization and dielectric constant which change with temperature. Its resistivity is high enough to permit charge storage. Pyroelectricity exists in polymers, and all pyroelectric materials exhibit piezo-electricity but not vice versa.

The measured sensitivity of such an image converter was reported as 10^{-3} W/cm². Its sensitivity increases with the frequency (proportion to f^2), while piezoelectric transducers are less sensitive at higher frequency. There is no resonance effect and hence it has a wide frequency band (just like all thermal detectors (thermocouples, thermistors, etc.), but which have never been used because of their extremely low sensitivity).

2.9 Electrostatic Transducer^(43,44)

This is a foil-electret transducer array for real-time acoustical imaging. The foil-electret microphone principle is employed to construct a two-dimensional transducer array. In one design, the back plate is divided into NxN elements, and one electret foil. The second design utilizes a back plate and an electret foil each with N strips of

metallization arranged in an overlapping fashion. Parallel sampling is done with the first design only. A 256 x 256 element array has been constructed,⁽⁴³⁾ having an area of $(256 \times 256)\text{mm}^2$, operating at frequencies 0.5 to 2.5 MHz. The elements were commuted at a frequency of 4 KHz so that 16 frames per second was delivered and real-time viewing was obtained. Acoustic holograms were obtained in less than 50 secs. at a frequency of 3.5 MHz, having a dynamic range of 35 dB.

Such electrostatic transducer arrays are used either in air or in water. The optimum frequency range in air is 70 to 250 KHz and in water, 0.3 to 3.5 MHz depending on the medium attenuation of the angular field of view. The sensitivity of this system was calculated to reach 10^{-8} W/cm^2 in air and $2 \times 10^{-11} \text{ W/cm}^2$ in water, but measured sensitivity was reported as 10^{-3} W/cm^2 only. Eighteen cm demountable sealed image converters of the Sokolov type were built with such a foil-electret transducer array as face plates.⁽⁴⁴⁾

2.10 Piezoelectric Array With Electronic Focussing and Scanning⁽⁴⁵⁻⁵⁰⁾

The use of a piezoelectric face plate in an acoustic imaging converter (Sokolov type) was discussed in the preceding section 1.6. Such large piezoelectric plate has a very limited angular field of view. This field of view increases with the decrease of the material size and reaches a very large angle when it is of the order of a mm or less. Thus an array or a mosaic of piezoelectric material will possess a large angular field of view together with high sensitivity (10^{-11} W/cm^2).^{*}

* Of the many available piezoelectric materials (quartz, lithium sulfate, barium titanate, lead zirconate-titanate, lead metaniobate, etc.) lead metaniobate is highly recommended because it has a very wide bandwidth without resorting to elaborate backing and matching, and it has minimum electrostatic coupling as compared to other materials.

A phased piezoelectric array in one or two dimensions has been designed for use in NDT B- or C-scan reflection mode or C-scan transmission mode. When such an array is electronically focussed and scanned in one direction only, the scanning in the other direction is done mechanically. Also, the same piezoelectric elements are used to both transmit (insonify) the object and receive (detect) the acoustic signal. Such a scheme has the advantage of having smaller aperture for the same definition (resolution), or better definition for the same aperture. Its image does not suffer from the speckle noise (because of the chirp property of the scanning scheme), nor from interference fringes at the image boundaries. The focal length of the array can be easily changed to any depth in the tested material. It has a faster rate of scanning (about 30 frames per second) in real-time operation. It also has a range gating with definition comparable to its transverse definition.

A schematic diagram of acoustic imaging system in one dimension is shown in Figure 7. It shows the piezoelectric transducers (PZT-5, 1.2 mm wide) receiving the acoustic image, and the BGO (Bismuth Germanium Oxide substrate) acoustic wave surface delay line, which provide the delay necessary in sampling the transducers array. For detailed discussion of the theory references (49), (46) and (45) are recommended. Arrays of 100 elements, measuring 11.75 cm, were built with acoustic BGO delay line having a corresponding 100 taps (one tap per transducer) with 50 MHz chirp frequency. This was used for acoustic imaging; using 1.6 to 2.5 MHz produced images with resolution about 1 mm. Objects used were 2-25 cm Al block with holes of various sizes; others were bonded Boron fiber reinforced epoxy laminate laid down on titanium. A

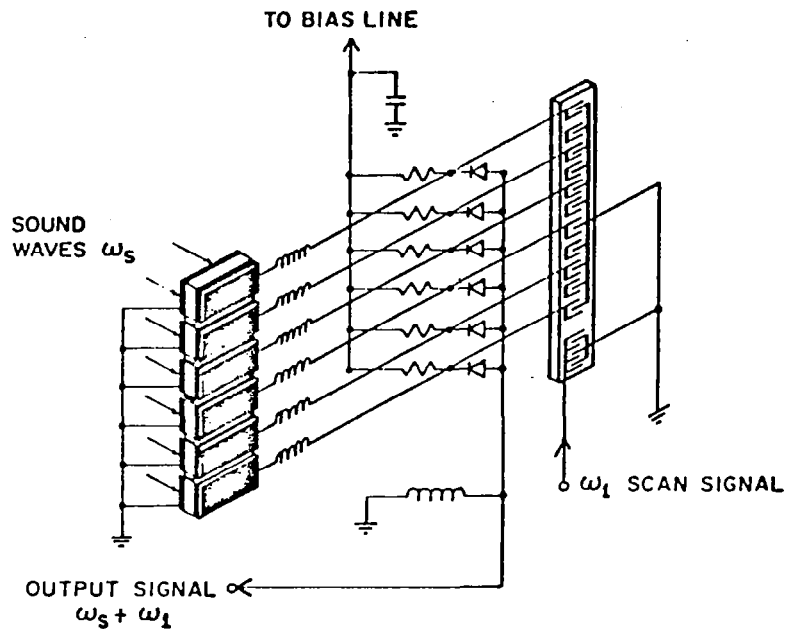


Figure 7. Schematic diagram of the essential elements of one dimensional acoustic imaging system, utilizing an array of piezoelectric transducers, electronically focused and ASW scanning. Such an array records an acoustic image much the same as photographic film in recording an optical image. A series of equally spaced taps is placed along the delay line and fed with the scanning frequency ω_l . Each tap corresponds to an individual transducer which receives the acoustic wave (frequency ω_s). Signals are mixed by simple diodes, and the output signal is the sum and difference of the two frequencies. The electrical imaging output of the device is received at one of these two frequencies.

third sample was cracked plastic with part of the crack filled with H_2O .

This technique seems to be one of the best and most sensitive techniques for nondestructive testing in real-time operation. It is similar to the ultrasonic probe used in the medical field, where 5x5 mosaic elements of lead metaniobate, measuring $(4 \times 4) \text{ mm}^2$ is designed for heart diagnosis. It operates at 3.5 MHz with 1 MHz bandwidth, and uses integrated circuits.⁽¹⁰⁸⁾ Arrays of 32x32 with element spacing of 1 mm are in the developing stage. There is no reason why such probes cannot be used in nondestructive probing of materials for the detection of voids, flaws, cracks, bonding, etc.

2.11 Frequency Swept Holographic Imaging⁽⁵¹⁾

In the previous section, a two dimensional array is used to angularly scan a probing narrow beam in object space and the received backscatter is used to generate a display of the relative positions and strengths of the various scatterers present. It is an excellent but expensive technique. Another cheaper method of mapping the scattered field utilizes only one transmitter and one receiver. The illuminating acoustic frequency is changed, causing the diffraction pattern (or hologram) of the object to expand or contract and swing in space with the object forming the center of gyration for the swinging and changing pattern. A single stationary receiver can be used to map the variation in the diffracted pattern as the pattern sweeps over it as a result of frequency sweeping the object illumination. Theoretical analysis of this frequency swept scanning technique shows that under certain conditions, the collected data is equivalent to that obtained from a linear scan of a receiver over the stationary diffraction pattern.

Lateral resolution is mainly determined by the width of the frequency sweep employed and the angle between the transmitter and the receiver observed from the object position. For example, it has been estimated that a resolution of 2 mm is expected for an acoustic system having (1-5) MHz frequency sweep with a transmitter-receiver angular separation of 60° . The range resolution is determined, in the case of chirped frequency sweep illumination, by the chirp rate and bandwidth of the post mixer. Range is changed by simply changing the chirp rate.

No experimental results have been reported yet.

2.12 Zone-Plate Acoustic Imaging Devices ^(52-56,17)

Both amplitude and phase zone-plates with PZT-4 and PZT-5 transducers were used to produce acoustic images in real-time. The experimental arrangement is shown in Figure 8 which is self-explanatory. They have been used with 10 MHz acoustic illumination, producing image resolution of 0.27 mm (about $1.8 \lambda_s$).

The amplitude zone-plate transducer, shown in Figure 9(a) is made of a gold zone-plate deposited on one face of a piezoelectric transducer. The other face of the transducer is coated with a uniform gold electrode. A voltage applied across the transducer activates the areas under the zones only and hence produces a focussed acoustic beam. With mechanical movement of the object, the transducer (focussed onto the object) can map the object point by point.

The phase zone-plate transducer is made by first applying a D.C. poling voltage across the amplitude zone plate in such a way as to reverse the original poling (of the transducer) between the zones, as explained in Figure 9(b). The gold zone-plate is then removed from the

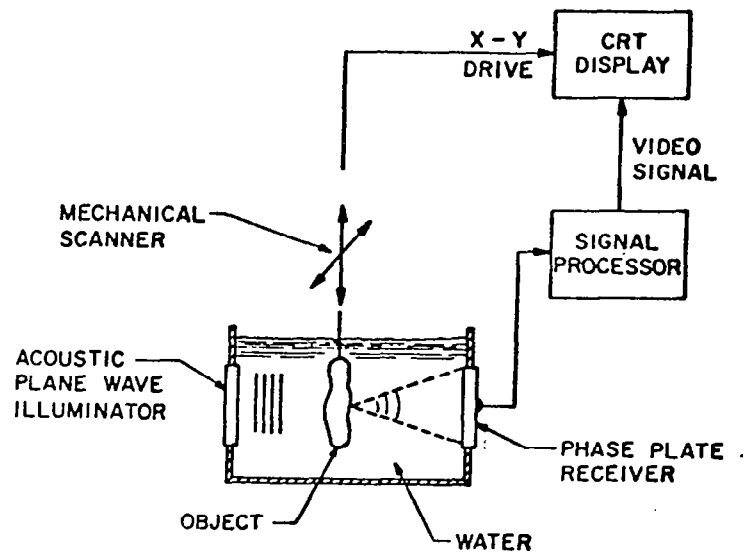


Figure 8. Operating arrangement for Zone-plate acoustic imaging devices.

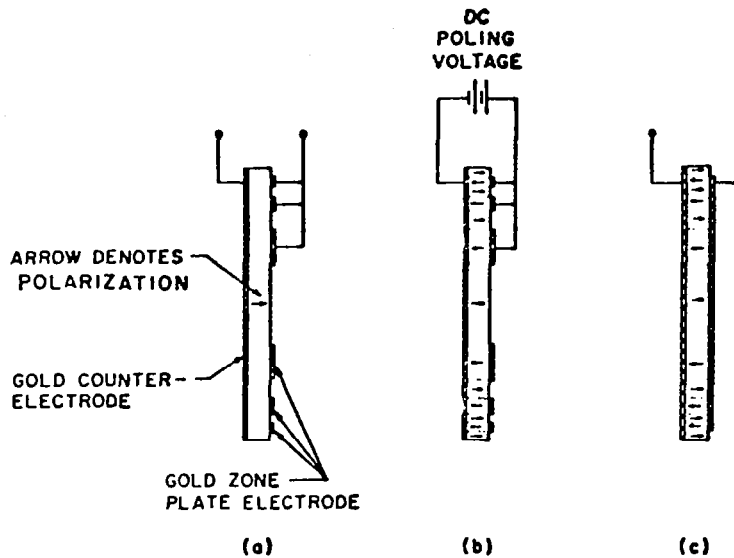


Figure 9. Fabrication of zone-plate transducers. The amplitude zone-plate transducer (a) is formed by depositing gold zone-plate pattern over the transducer. The phase zone-plate transducer is formed by first determining the PZT polarization and then applying a DC poling voltage (as shown in (b)) to reverse the polarization in zones between the zone-plate electrode and its counterpart. Finally, the gold zone-plate is replaced by a simple disk electrode (as shown in (c)) over the phase zone-plate pattern.

face of the transducer and is replaced by a uniform electrode to form the finished phase zone-plate. The focus of such a plate depends on the frequency which gives it an added flexibility of axial scanning.

Such zone plate transducers can be used as both transmitters and receivers. Wade and his co-workers^(54,55) used a different scheme, utilizing the optical projection of a Gabor type zone-plate pattern on a composite transducer. The transducer is a sandwich structure (shown in Figure 10) containing a piezoelectric layer which is differentially activated via a photoconductive switching. Such an optical-acoustical transducer is addressed by light carrying an acoustic zone-plate pattern which is projected on the photoconductive layer. In absence of light, most of the voltage drop is across the photoconductor; with the light on, the resistance drops and therefore the voltage is applied across the piezoelectric transducer, producing a replica of a zone plate pattern of an acoustic source.

A variation of this scheme [shown in Figure 10(b)] uses a dielectric on the top of the photoconductive layer. This results in an opposite operation; i.e., when the voltage is on and the light is off, strong acoustic radiation is emitted, and with the light on, we get a negative pattern of the zone-plate.

Devices based on this principle are in the laboratory stage; they are designed to operate near 3 MHz. The transducer focal length is 10 cm and its diameter is 12 cm.

2.13 Gabor's Sonaradiographic Imaging Scheme⁽⁵⁷⁾

Focussed holograms have the advantage of the amplifying effect of the reference beam, but they have the disadvantage, which always arises

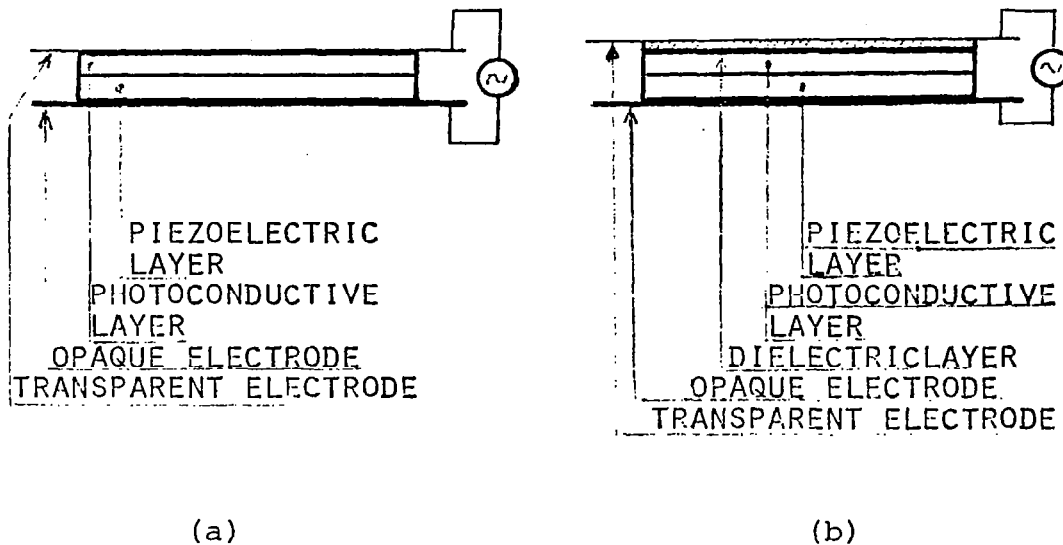


Figure 10. Zone-plate transducers utilizing projected light zone-plate of Gabor type. (a) is the positive type operational configuration; it consists of a transparent electrode on top of a photoconductor (CDS) which is in contact with the piezoelectric transducer (LiNO_3 or BaTiO_3). (b) is the negative type operational configuration; when the electric voltage is on, then in the dark strong acoustic radiation is emitted; this radiation is stopped when the light is switched on, thus, giving a negative Zone-plate pattern.

in the case of coherent sound, of very strong speckle noise.

To eliminate this speckle noise, acoustic imaging should use one of the following techniques:

- (a) Incoherent acoustic waves.
- (b) Cut out all the sections other than just the one from which the signal is detected. This can be accomplished by the electronic focussing and scanning (section 1.10) or zone-plate devices (section 1.12).
- (c) Sonaradiography (as outlined below) where only one section in the depth of the object is isolated and imaged.

The scheme proposed by Gabor is based on producing holograms with very short single acoustic pulses. When such a pulse is scattered by a point object, the scattered wave will produce on an intervening membrane a rapidly spreading ring-shaped fine ridge. If then we illuminate the membrane with a high frequency stroboscopic laser light source for a short interval, the trace of the spreading ring will appear exactly like the hologram of a point object (a system of Fresnel zones), which can then be photographed and reconstructed. By proper gating we can then make holograms of any section within the object. Since the acoustic pulse used for illumination is very sharp, no speckles will appear in the hologram.

This scheme was intended for use in medicine, but there is no reason why it cannot be used for industrial NDT. Unfortunately, the work on this idea was terminated without satisfactory conclusion.

2.14 Acoustic Tomography⁽⁵⁸⁾

Tomography (well known among x-ray radiographers) is the technique by means of which a sharp image of one section of the object is obtained by moving the illuminating source and the recording plane in opposite direction. The section to be imaged depends on the relative positions of the source, the object and the recorder. This technique is well known among medical diagnosticians, but we believe that it can be extended to material NDT. However, careful study of such a possibility has not been done during the course of this contract.

2.15 Piezoresistive Image Converter^(59,60)

One difficulty with the piezoelectric face tube (Sokolov type, section 1.6) is the lack of extended grey scale in the image. It is difficult, with these tubes, to present more than 5-10 distinct shades of grey. To overcome this difficulty, piezoresistive materials [like CdS (Cu)] may be used. Such materials have a wide range of acoustic frequencies as opposed to the resonant frequency and odd harmonic response of the piezoelectrics. They also have high resistivity and have the capability of information storage, since the piezoelectric transducer presents to the scanning electron beam a signal proportional to the acoustic intensity incident at the moment of scan, while the storage system (using piezoresistive transducer) presents all the accumulated signals since the last scan. This can then lead, in theory, to significant improvement in sensitivity, in addition to the freedom to use pulsed acoustic illumination. Sensitivity of the order of 10^{-7} W/cm² has been reported.

2.16 Electroluminescent Acoustic-Image Detector⁽⁶¹⁾

Such a detector combines a piezoelectric and electroluminescent layers in contact, as shown in Figure 11. The thickness of the electroluminescent layer, together with proper simulation for luminescence such as bias voltage or UV illumination, are important in yielding a phosphor which could be stimulated by the piezoelectric voltage generated. Threshold sensitivity in the order of 10^{-6} to 10^{-7} W/cm² has been reported. However, activities in this field are practically at a standstill.

2.17 Photographic and Chemical Direct Acoustic Recording^(61,62)

Although none of the direct recordings of acoustic images by photographic or chemical recording are presently in use (mainly because of their relative low sensitivity, which is of the order of 1 W/cm²) they are briefly surveyed in this section since they were part of our study. Hereunder is a summary of our findings based mainly on ref. (62).

Ultrasound can be detected by means of the direct action of ultrasound energy on a photographic emulsion and because ultrasound accelerates or causes some chemical reactions. The fact that ultrasonic radiation influences a photographic emulsion was reported in 1933 by Marinesco and Truillet⁽⁶⁴⁾. Subsequent studies by other investigators still have not clearly revealed the exact mechanism involved. The analysis by Bennett⁽⁶⁵⁾, in which he showed that luminescence and pressure effects did not appear to explain all the existing facts, remains a good discussion of this situation. Although Bennett indicated rather conclusively that the softness of the photographic emulsion was a very

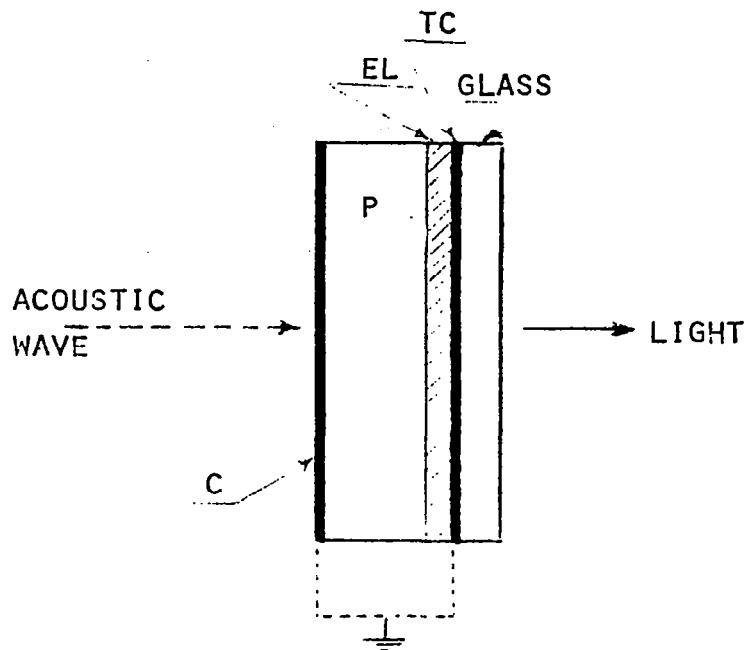


Figure 11. Piezoelectric electroluminescent phosphor image detector. The voltage generated across a thin electroluminescent phosphor layer (EL) by the action of acoustic wave impinging on a piezoelectric material (P) would stimulate light emission which could be observed through the transparent electrode (TC) and a glass support plate. The (TC) electrode on the phosphor is connected to the (C) electrode on the piezoelectric material; voltages generated on the piezoelectric material appear at the interface with the electroluminescent layer.

important factor in its response to ultrasound, he stated in his conclusion that "there is not sufficient evidence to delineate clearly the mechanism, whether thermal, mechanical or otherwise". Bennett's work did indicate that the photographic speed of the film emulsion had little effect on the result (his tests included film speeds for tungsten from less than 10 to 160).

The softness of the emulsion has been shown to be a significant factor for the film detection of ultrasound. Film exposed in the dark to ultrasound and developed in the normal manner will yield a useful image with an exposure time of about 4 hrs for an ultrasonic intensity of 1 W/cm^2 . If the temperature of the film is raised from 20° to 28°C , a significant exposure improvement factor can be obtained. If the emulsion is soaked in water at room temperature prior to exposure, a factor of about four times less exposure can be used⁽⁶⁶⁾. Both these improvements were reported to be based on the fact that the emulsion was softened.

These photographic film methods of course require darkroom techniques. There are other photographic methods which do not. One involves the ultrasound exposure of film in an iodine solution⁽⁶⁶⁾. The effect of the ultrasound exposure on the emulsion is to render the emulsion resistant to fixing to an extent proportional to the exposure. The image becomes visible during the exposure because the emulsion turns a darker yellow color.

The image can be made visible more easily after completion of the exposure by fixing the film for a short time (for example, 1 min in Kodak liquid X-ray fixer and replenisher) in order to clear the unirradiated

emulsion. The remaining emulsion then displays the sound pattern by a yellow color against the clear background. Those areas of greatest exposure remain essentially yellow, while in areas of intermediate exposure the emulsion is partially cleared. There is therefore some grey scale in the image. This detection method can be used in the light since the exposed film is not developed and light appears to have little influence on the fixing of the emulsion.

A second photographic method which can be performed in the light involves the ultrasound exposure of photographic film or paper in a developer solution^(67,68). The uniformly light-exposed emulsion develops more quickly in areas where the ultrasonic intensity, and therefore agitation of the developer, is highest.

A thorough study of this technique with photographic paper has been made and reported by Arkhangel'skii and Afanas'ev⁽⁶⁸⁾. They found that one could obtain a maximum paper density contrast in the exposed areas for a developer concentration of 0.2, an exposure time of 90-110 sec, and an ultrasonic intensity of 0.15-0.25 W/cm² for photographic paper No. 6. The threshold sensitivity was reported to be 0.05 W/cm² for a high developer concentration and an exposure time of 40 sec. Exposure times could not be too long or the paper would develop completely.

A practical aspect of the developer and photographic paper study by Arkhangel'skii and Afanas'ev is that they devised a thin detector cell containing developer solution and paper. The cell had ultrasound transmitting windows of thin (0.15 mm) rubber and allowed a space of 2 mm inside the cell for the paper and developer solution. In this manner the need for a large tank containing developer solution as the exposure

tank was eliminated.

The same authors also studied the resolution characteristics of the photographic paper method. The resolution is determined by the transverse diffusion of the developing solution in the photolayer and by the presence of nonuniform streaming. This latter effect leads to distorted and by the presence of nonuniform streaming. This latter effect leads to distorted images because fresh developer is directed along the ultrasonic field by the acoustic wind. The rubber-covered detector cell tended to eliminate some of this problem. Assuming that the streaming problem could be eliminated, the authors indicated that the resolution of the detector could be in the range of 0.01 mm.

One chemical detection method that has been studied by a number of investigators involves potassium iodide-starch solutions^(69,70,71-73). Under ultrasonic irradiation air-filled water undergoes an oxidizing reaction to form H_2O_2 , which tends to discolor organic dyes. For example, the potassium iodide-starch solution tends to turn blue. Rust et al.⁽⁷¹⁾ used this phenomenon to detect ultrasound images by making an array of boxes containing this solution. Each liquid-filled box tended to darken depending upon the ultrasonic intensity. Darkening also depended upon the iodine concentration and the exposure time.

The individual liquid-filled boxes had to be at least one wavelength in depth for optimum results. The threshold ultrasonic intensity was reported to be $0.5-1.0 \text{ W/cm}^2$. At that intensity exposure times were only about 2 min. The threshold intensity could be lowered to a value as low as 0.07 W/cm^2 if small amounts of aliphatic chlorides such as CCl_4 or chloroform were added to the solution⁽⁷⁰⁾.

A similar method suggested by Bennett⁽⁶⁹⁾ called for the exposure of films of starch on glass plates in an iodine solution. Here too a blue color was produced in areas of higher ultrasound intensity. Exposure times of about 2 min at 1 W/cm^2 were common.

A number of other chemical techniques involving more complicated organic dyes have also been investigated^(74,75). Recently, a new photopolymer material for optical hologram recording was announced^(76,77). It is grainless, exhibits 100% diffraction efficiency, irreversible, can be overmodulated, no wet processing is needed, and permits the diffraction efficiency to be preadjusted for a variety of desired angular responses and spatial frequencies. It is, however, not very sensitive (slower than 649F emulsion) and displays poor low spatial frequency response. The material is photopolymerizable, sensitized in the blue-green spectral region with a dye sensitizer; thus it can be exposed for all the argon-ion laser wavelengths. It can be coated on glass or film base with thickness from a few micrometers to several hundred micrometers. A typical hologram was recorded on this material with 3:1 reference to object beam ratio, in 30 seconds using 12.8 mW/cm^2 .

The material is still under development and is being tested in various optical laboratories.

However, nothing is known about the response of this material to acoustic radiation or electron beams. Thus its use for acoustic recording seems at the present to be limited to systems where the acoustic image is converted to an optical image (first as, for example, in Gabor's scheme, or with piezoelectric-electroluminescent devices, etc.). However, with its present low speed characteristic, it is doubtful that it has use

in acoustic image recording, except in special cases.

2.18 Solid and Liquid Crystal Acoustic Displays⁽⁷⁸⁻⁸²⁾

Crystalline solid, thin layer of $\text{CoCl}_2 \cdot 6\text{H}_2\text{O}$ was used to demonstrate its capability to visualize acoustic images. The concept is based on the well known fact that acoustic waves projected on a suitable absorbing material is converted into a corresponding thermal map of the acoustic image. Since the color of cobalt chloride crystal layer depends on its crystal structure, and this is a function of its local temperature, different ultrasonic intensities show up in various colors, starting from pink, then blue, and ending in white. The interest in such solid crystals as acoustic field detectors has been only an academic curiosity.

On the other hand the interest in liquid crystals is more than academic. It is practical and progressive development of these crystals and their potential use as real-time acoustic image display devices is carried out in various laboratories. The optical properties of these crystals resemble those of crystalline solid.

Liquid crystals are usually divided into smectic, nematic and cholesteric, depending on the arrangement of the molecules and their degree of rotational freedom. Only the nematic and cholesteric types were used as acoustic to optic converters. Several cholesteric materials were tried as acoustic area detectors. These attempts were based on thermal mapping of spatial temperature variation on an ultrasonic absorber irradiated by the acoustic field⁽⁷⁹⁾. Most of the problems with cholesteric liquid displays is that they have limited resolution (which is a function of the thickness of the substrate) and poor sensitivity. Microencapsulation in coating materials of high acoustic

properties and using an acoustic impedance close to that of the encapsulated cholesteric liquid crystals has been suggested to improve the resolution. Ultrasonic holograms were recorded with cholesteric liquid crystal area detectors, by properly thermal balancing of the liquid crystals, and by using a transparent acoustic absorber in specially constructed black bottom tank⁽⁸⁴⁾. In spite of such demonstration of the use of cholesteric liquid crystals in acoustic holography, such method is more of a scientific than a practical importance, since the acoustic intensity used was 8.1 W/cm^2 at a frequency of 5 MHz. Improvement of the sensitivity (may be by an order of magnitude) would, however, mean the need for an ambient temperature regulation to 10^{-3} degrees which rules the scheme out for any practical use.

Better schemes for using liquid crystals exploit the five electro-optical effects which have been observed in certain types of nematic liquid crystals, all of which may perhaps be influenced by an ultrasonic field. Based on these electro-optical effects, the following suggestions were made to design liquid crystal displays.

2.18.1 Dynamic Scattering

When an electric field is applied, the liquid crystals become milky white and opaque. This dynamic scattering is due to the interaction of charge carriers and the dipole moment of the nematic liquid crystal molecules. Since ultrasonic fields influence the electric conduction, the dynamic light scattering may be affected and the changes taking place could be used for acoustical imaging displays⁽⁷⁸⁾.

2.18.2 Voltage Controlled Optical Activity

A thin layer of twisted nematic liquid crystals is sandwiched between two glass plates, each provided with conductive coating. The molecules of the liquid crystals are turned 90° in going from one glass plate to the other with no electric field applied. When linearly polarized light is incident perpendicular to one side, its plane of polarization will rotate along the twist axis of the nematic molecule a total of 90° as the light is transmitted to the other side. On the other hand, when an electric field is applied across the cell, the liquid crystal molecules are rearranged so that their orientation no longer shows a continuous twist of 90° and so light will pass through the cell. Knowing that static electric fields and acoustic fields may interact, such interaction could be used to develop an acoustical-to-optical display.

2.18.3 Guest-host Interaction

A dichroic dye molecule is introduced as a "guest" into the crystalline "host" nematic liquid crystal. The orientation of the dye molecules and their optical absorption are controlled by applying an aligning electric field. Since the optical absorption properties of certain dyes are influenced by acoustic radiation, a real-time acoustical-to-optical display screen may be reconstructed.

2.18.4 Birefringent Properties

Phase deformation in vertically aligned liquid crystal (specially prepared) shows up in their light transmission properties, as was observed by Schickel and Fahrensohn of AEG-Telefunken. Contrast ratio of 1000:1 have been achieved using only 7-10 volts. The orientation of the liquid crystals can be influenced by an acoustic wavefront and hence the latter may be visualized.

It is to be emphasized that none of the above suggested schemes have been tested.

Other tested schemes are presented below.

2.18.5 Direct Acousto-Optical Effects⁽⁷⁸⁾

Propagation of acoustic waves in nematic liquid crystals causes turbulent motion of these crystals, and this leads to dynamic optical scattering in the liquid crystal layers (in the absence of any electric field). This was demonstrated⁽⁷⁸⁾ by bonding an array of 10 MHz PZT-4 acoustic transducer to the back of a liquid crystal cell. When the transducers were switched on, the liquid cells in contact with them turned milky.

It was found that the sensitivity of such a cell can be increased by proper biasing with an electric field⁽⁸⁵⁾. Appendix A, pp. A-13 describes a successful design of such an acousto/optic liquid crystal display screen⁽⁸⁰⁾.

Although image quality of liquid crystal devices are quite poor, the existing interest in such devices is motivating many researchers to pursue their work with optimism.

New results will be reported at the Acoustical Holography Symposium #7 at Chicago, Illinois (August 1976) by J. L. Dion, of Canada, on the use of homeotropic nematic liquid crystal cells having sensitivity better than 10^{-6} W/cm² independent of the frequency in the range of 1 to 10 MHz.

2.19 Pohlman Cell^(86,87)

This cell is described in Appendix A, pp-13. Pohlman announced the idea in 1939⁽⁸⁶⁾ and then demonstrated its use in 1948⁽⁸⁷⁾. To improve the contrast of acoustic images detected by these cells, Van Valkenburg⁽⁸⁸⁾ applied a small bias voltage (typically 25-30 V AC) across the cell. The voltage tends to align the flakes so that no light is reflected in the absence of ultrasound. Results were shown⁽⁸⁸⁾ using 5 MHz. Such cells, however, gave way to other techniques of acoustic imaging, because of its poor relative resolution and sensitivity (10^{-1} to 10^{-3} W/cm² with reaction time ≤ 1 sec., and 2.8×10^{-7} W/cm² with expected reaction time of the order of minutes). It also has a limited dynamic range of 20 dB.

2.20 Oil, Thermoplastic and Photoplastic Films^(88,89,90,110)

All these detectors are used after converting the acoustic image into an electronic one and focussing the electrons on one of these materials.

A thin oil film is used to coat an optically flat glass plate in vacuum. The electrons, writing on the oil film, are attracted by a high voltage on the glass plate, causing the oil surface to deform, which in turn results in varying the thickness of the oil film. The deformed film is then read out optically by using a phase modulation scheme, and an optical image is projected.

Thermoplastic film is very similar to the oil film. A thin layer of low-melting-point plastic is coated on a transparent conducting film. The film is written on by an electron beam and heated to the softening point of the plastic coating. The electrons are attracted by a high voltage on the conducting backing and produce thickness variation in a manner similar to that of the oil film. After cooling, the plastic hardens, and thus a permanent record is available.

Photoplastic is very similar to thermoplastic, except that it is also a photoconductor. The surface of the photoconductor is charged, and, at points where light strikes the photoconductor, the charge leaks through to the conducting layer on the base. The remaining charge causes deformation when the photoplastic is softened by heating in the same way as with thermoplastic. This material is better than the thermoplastic because it does not require vacuum; however, it is less sensitive.

All of these materials require complex and expensive material in addition to their low sensitivities $0.1 - 1 \text{ W/cm}^2$ and hence they cannot compete with other detectors.*

* For recent advances, see Ref. B.

2.21 Scanning and Sampling Technique⁽⁹¹⁻⁹⁵⁾

Historically the first acoustic holograms were recorded (either in air or water) by scanning a small microphone (in air) or piezoelectric detector (in water) over the hologram plane. The signal then modulates the intensity of a CRT electron gun, or a small neon bulb focussed on a photographic plate. The CRT electron beam or the neon bulb move in synchronism with the acoustic detector at a slow speed to produce an optical hologram properly demagnified. There have been a variety of arrangements of this technique, one of which gives a sampled hologram which can be constructed by a computer⁽⁹⁶⁾, another by keeping the detector stationary and scanning with the insonifying source (what is known as reciprocal hologram^(104,104)), a third by scanning both the source and the detector simultaneously with the same or different relative speed to produce a synthetic aperture hologram^(105,106), a fourth approach produces a phase only hologram⁽¹⁰⁷⁾, etc.

The literature is full of such techniques. The scanning is done mechanically and thus it is very slow and for this particular reason it is rarely used. However, if a mosaic of detectors are made to sample the field in parallel, then it can produce a hologram almost instantaneously. However, the reconstruction or computer data reduction limit the speed of the process to obtain the final visual image. Such schemes are superceded presently with the more sophisticated techniques described in previous sections (e.g., electronically focussed and scanned piezoelectric transducers, Bragg cells, rippled surface, etc.).

2.22 Recent Developments (yet to be published)*

Takuso Sato used a rotating random phase disk behind the object to detect the signal by a fixed receiver placed far from the disk, thus transforming the spatial distribution of the wave intensity of the object waves to be reconstructed into a temporal distribution. This idea eliminates the need for a scanning receiver or phased array receivers.

Hitachi Ltd. of Japan will announce soon a shear wave focussed image holography system for sizing vertical and oblique flaws and defects in metal structures. The system utilizes acoustical holographic interferometry in the focussed image hologram mode. The image of an internal flaw consists of interference fringes or contour lines across the flaw's surface. The fringe separation represents half wavelength deviation in depth from the scanning plane, and the length of the fringe corresponds to the width of the flaw. Thus one can estimate the size of the flaw by measuring the number and length of the fringes which appear on the focussed image hologram.

In an effort to suppress the effects of object vibrations, changing temperature, and other external influences, H. J. Shaw applies the principle of differential phase contrast imaging where comparison is made between the phases of adjacent points on the object, which are separated by a constant distance along the scan line. This is different from the fixed reference phase contrast imaging in that the reference and signal beams travel almost identical paths.

*

It is expected that some of these accomplishments will be announced at the Acoustical Holography Symposium #7 (Aug. 1976).

Real-time imaging with shear waves and surface waves, using the FM chirp focussed phase array and tilting the array past the critical angle for longitudinal waves in the target block, shows a 5 mm definition in the normal direction and 4 mm in the horizontal direction at a distance of 15 cm in an Al block, when the acoustic frequency was 1.8 MHz. When the array is tilted further than the critical angle, exciting Rayleigh waves, the resolution achieved did not change. This information was obtained from G. S. Kino.

CHAPTER III

ANALYSIS, CONCLUSIONS AND RECOMMENDATIONS

3.1 Image Quality

Acoustic images produced by whatever technique are far inferior to optical images. They are not as sharp, reveal poor resolution, distortion, noisy, and can lead to erroneous interpretation. However, they do reveal the internal structure of the object, and not merely its outside surface. In comparison with x-rays, they are again, as a whole, of less quality; but again because of the nature of interaction of acoustic waves in the materials they give information about the interfaces in the tested objects, which are hidden or not evident in x-ray pictures.

Hereunder are the main causes for limiting the quality of acoustic images.

(a) Wavelength. Acoustical frequencies (normally used for non-destructive testing (0.1 - 20 MHz) are far below the optical frequencies ($\sim 10^{14}$ Hz). Naturally, then, the acoustic resolution is less than optical ones. Indeed, images obtained in acoustic microscopy where very high frequencies (1 - 10 GHz) were used, compete very well with optical microscopy pictures.

(b) Specular Reflection. Most of the surfaces are smooth relative to the acoustic wavelength. This produces specular reflection and hence false interpretations. For example, rods may look like wires, spheres as points, etc. Thus, care must be taken in choosing the right acoustic frequency to insonify the object, relative to its surface roughness, geometrical arrangement, etc.

(c) Speckle Noise. This is produced by the coherent nature of the irradiation. It can be eliminated by using wide frequency band, large

aperture, very sharp pulsing for insonification, large aperture, and/or focussed detection.

(d) Limited Aperture. In reconstructing an acoustic hologram with visible light, the hologram dimension must be reduced by the ratio of the acoustical wavelength to optical wavelength (Appendix A, pp. A-4) which is of the order of magnitude of 1000; otherwise, depth distortion is generated in the reconstructed image. A highly reduced hologram on the other hand will be too noisy due to speckles. Other means to avoid the demagnification of the acoustic hologram under reconstruction, and produce an undistorted image, are (a) the use of composite holography (discussed next); (b) ignore the depth information; or (c) resort to direct focussed imaging (item 1.10, for example).

(e) Depth Distortion. One of the main attractions to holography is to reconstruct the whole 3-D information about the object from one hologram. However, when there is a change between the wavelengths of the radiation used in recording and reconstructing the hologram, the depth of the object (in the reconstructed image) is magnified or demagnified relative to the other dimensions of the object. To avoid this the hologram dimensions have to be changed (as explained above and Appendix A, pp. A-4). This, however, may be undesirable.

Another idea to obtain undistorted depth information, separate images are made for various sections in the body (e.g., using a B-scan). Transparencies of these images are then stacked and one optical hologram of the whole stack is made optically^(97,98). This hologram then may be reconstructed later with the same optical wavelength, to produce an undistorted visible acoustic image of the object.

(f) Miscellaneous Artifacts. Interpretation of acoustic images is sometimes hampered by artifacts peculiar to the technique used. Scanning, for example, whether linear, circular or helical, may produce moire patterns⁽⁹⁹⁾, multiplicity of images which are not separated from one another, etc. Diffraction fringes may appear to hinder the location of sharp edges. Speckle noise may be confused with the roughness of the surface.

3.2 Comparison of Various Techniques.

The various systems for visualizing acoustical images in NDT are described in Chapter 2 and summarized in Table 1. They are also presented in a condensed form in Appendix A, Table A.I, pp. A-6. The choice of a proper system depends on:

- (a) type and size of object to be tested,
- (b) accessibility to the object (i.e., tested on site or in the laboratory),
- (c) degree of the details of the information,
- (d) need for real-time information, or a record for filing,
- (e) need for gross macroscopic information only, or gross and fine microscopic details,
- (f) whether the system is to work alone or as a complement to other systems,
- (g) whether the system has the capability of acoustical imaging only or both acoustical and optical imaging, and
- (h) the cost of the system.

The Bragg-diffraction system (Section 2.3) exhibits the capability for real-time acoustic image visualization, and at the same time with some modification, can be switched to real-time optical imaging. It is simple and sensitive enough. However, it may be limited to testing of medium sized objects which can be moved to the lab and placed in the water filled Bragg cell.

For macroscopic and microscopic testing of medium sized objects, an electronically focussed, electronically scanned piezoelectric array (Section 2.10) offers the best technique at the present.

For large objects, a piezoelectric mosaic array may be built as a probe to scan the object mechanically (like a stethoscope). This is similar to the technique used in medical diagnosis. Like the above two techniques it has the capability of real-time display.

Most of the other techniques have not yet proven their practicality, are still in the research or development stage, or incapable of real-time display.

With the exception of Sokolov-type image converter system (Section 2.6) and the deformed water surface (static ripple) system (Section 2.2), no other system is available commercially. Both systems, however, have limited field of view.

3.3 Recommendations.

1. Follow up the international state of the art and new development in this fast moving acousto/optical imaging technique.

2. Design an acoustical system, or systems, that can be incorporated in the MSFC hybrid system (Figure 1), according to the types of objects to be tested.

3. Analyze and design the whole hybrid system for nondestructive testing incorporating optical, acoustical and correlation techniques. This includes information acquisition, storage, reduction and retrieval in addition to the various subsystems of imaging, rectification, enhancement, etc.

4. Study and build a portable probe for testing large objects on site, akin to that used in medical diagnosis (utilizing integrated circuits⁽¹⁰⁸⁾).

5. Initiate a program to study microscopic cracks and monitoring them acoustically.

6. Initiate a study program on zone-plate acoustic imaging devices with the possibility of using the zone-plate for both acoustical and optical focussing.

7. Investigate more thoroughly the capabilities of acoustic tomography (Section 2.14) and Gabor's sonoradiography (Section 2.13).

TABLE 1

ACOUSTO/OPTIC IMAGING METHODS AND DETECTION

Imaging System	Detectors or Detection Technique & Display	Real-Time Capability	Sensitivity W/cm ²	Frequency Range MHz	Section Reference	General Remarks
Liquid Surface (static ripples)	Optical phase contrast or optical scanning with coherent or incoherent light	Yes	1.5x10 ⁻³ (normal) 10 ⁻⁵ (reported) 10 ⁻⁹ (theoretical)	0.5-10	2.2	
Bragg-Diffraction (Direct sound-light interaction)	Coherent laser light (continuous or pulsed)	Yes	10 ⁻⁹ (theoretical)	10-100	2.3	
Deformed Solids (dynamic ripples)	Laser beam scanning or electron beam scanning	Yes	10 ⁻³ (reported) 10 ⁻⁹ to 10 ⁻¹¹ (theoretical)	100	2.4, 2.5	
Image Converter (Sokolov)	Scanning the back of PZT face (quartz or barium) electronically & detect secondary emission.	Yes	10 ⁻⁹ (theoretical)	Up to 0 or 20	2.6	Sealed tube -very narrow angular aperture (10-20°) -3λ _s -5λ _s resolution (reported) -new designs may increase aperture and frequency.
Metal Fiber Face tube image converter (with appropriate PZT)	Scanning the back of the PZT electronically (like Sokolov tube)	Yes	10 ⁻⁹ (theoretical)	Up to 20	2.7	Improves the angular field of view of Sokolov tube.

TABLE 1 (Cont'd)

Imaging System	Detectors or Detection Technique & Display	Real-Time Capability	Sensitivity W/cm ²	Frequency Range MHz	Section Reference	General Remarks
Pyroelectric face tube image converter	Pyroelectrics scanned with electron beam	Yes	10 ⁻³ at 3 MHz (reported)	Up to 20	2.8	-Sensitivity increases with f ² -wide frequency band (>20 MHz) -sealed tube
Electrostatic Transducers	Electric switching	Yes	10 ⁻⁸ in air } 10 ⁻¹¹ in water } (theoretical) 10 ⁻³ (reported)	0.07 to 0.250 in air 0.3 to 3.5 in water	2.9	
Piezoelectric array with electronic focussing & scanning	Electronic	Yes	10 ⁻¹¹ (theoretical) 10 ⁻⁸ (reported)	1-20 (used)	2.10	Laser beam scanning of PZT for readout has sensitivity of 10 ⁻⁴ W/cm ² .
Piezoresistive Image Converter	Electron beam scanning	Yes	10 ⁻⁷ (reported)	1 to 20 (used)	2.15	Has larger dynamic range than piezoelectrics.
Electroluminescent image converter	Direct conversion	Yes	10 ⁻⁶ (reported)		2.16	Has storage capability.
Photographic and Chemical Methods	Direct interaction	No	~1-5 (reported)	> 0.02	2.17	
Photopolymer materials	After conversion to visible or electron images	No	0.013 (reported) (with Argon Ion laser)		2.17	

TABLE 1 (Cont'd)

Imaging System	Detectors or Detection Technique & Display	Real-Time Capability	Sensitivity W/cm^2	Frequency Range MHz	Section Reference	General Remarks
Oil, Thermoplastic and photoplastic recorders	Electron beam scanners plus optical illumination	No	0.1-1 (reported)		2.20	
Pholman Cell	Direct Interaction	Yes	10^{-1} to 10^{-3} (reaction time 1 sec.) 2.8×10^{-7} (reaction time ~60 secs.)		2.19	Poor resolution, poor contrast, and limited dynamic range of 20 dB.
Solid and Liquid Crystal Display	Direct Interaction	Yes	$0.1-10^{-6}$ (reported)		2.18	Still in experimental stage.
Chemical Techniques Phosphor persistence changes.	Direct Interaction plus proper viewing system	Yes	0.05-0.1			See Ref. 102 which includes specific references; e.g., Ca-CrS stimulated by UV increases its luminescence persistence by acoustic exposure. Spatial resolution of 0.2 mm reported.
Extinction of luminescence			1			

TABLE 1 (Cont'd)

Imaging System	Detectors or Detection Technique & Display	Real- Time Capability	Sensitivity W/cm ²	Frequency Range MHz	Section Reference	General Remarks
Chemical Techniques (Cont'd)						
Thermosensitive color changes			1			Chromotropic compound (e.g., Hg·Ag·iodide); changes color from yellow to red instantly with acoustic absorption (1 sec. exposure); irreversible process.
Change in Photo- emission			0.1 (at 5 MHz)			
Change in electrical conductivity			0.1			Semiconductor materials such as zinc & cadmium.
Thermocouple and thermistor			0.1			Thermopile detects 0.1 W/cm ² , temp. rise of (10 ⁻⁴)°C.
Zone Plate Acoustic Focussing (on PZT)	Electron or Optical Scanning	Yes	10 ⁻¹¹		2.12	
Gabor's Sonoradio- graphy	Coherent laser beam & photo recording	No			2.13	No results reported.
Acoustic Tomography	PZT	No	10 ⁻¹¹ (theoretical)		2.14	Mostly used in medicine.
Frequency Swept Recording	PZT	Possible	10 ⁻¹¹ (theoretical)		2.11	No results reported.

TABLE 1 (Cont'd)

Imaging System	Detectors or Detection Technique & Display	Real- Time Capability	Sensitivity W/cm^2	Frequency Range MHz	Section Reference	General Remarks
Digital Sampling and Computer Reconstruction	PZT (in water) Microphone (in air)	No	10^{-11} (theoretical)		2.21	Slow
Rutican Recording Devices	Light image	Yes	30 ergs/cm^2		Appendix B	

BIBLIOGRAPHY

1. R. K. Mueller and N. K. Sheridan, App. Phys. Letters 9, #9, 238-329 (1966).
2. P. S. Green, Lockheed MSC, Rept. #6-77-67-42 (Sept. 1967).
3. Acoustical Holography Symposia Proceedings, published by Plenum Press, New York.
4. Ultrasonics Symposium Proceedings, published by IEEE.
5. R. L. Kurtz, App. Opt. 12 (12), 2815-2821 (1973); 13(8) 1771 (1974).
6. H. M. A. El-Sum, Acoust. Holog. 1:1-26, Plenum Press (1969).
7. H. M. A. El-Sum, Acoust. Holog. 2:7-22, Plenum Press (1970).
8. R. K. Mueller, Proc. IEEE 59: 1319 (1971).
9. P. Greguss, Phys. Today 27: 42 (1974).
10. G. Wade, private communications.
11. L. D. Rozenberg, Soviet Physics-Acoustics 1 (2), 105-116 (1955).
12. R. B. Smith and B. B. Brenden, IEEE 1968 Symposium on Sonics and Ultrasonics, New York City (Sept. 1968).
13. H. M. A. El-sum et al., Acoust. Holog. 1, Plenum Press (1969).
14. N. K. Sheridan, Acoust. Holog. 2, 275-288 (1970).
15. P. S. Green, Acoust. Holog. 3, 175, Plenum Press (1971).
16. J. B. Swint, et al., Acoust. Holog. 3, 163, Plenum Press (1971).
17. K. Y. Wang and G. Wade, private communication; Acoust. Holog. 4, 431-462, Plenum Press (1972).
18. A. Korpel, App. Phys. Letters 9, 425 (1966).
19. H. M. A. El-Sum, Acoust. Holog. 1, 22, 149-172, Plenum Press (1969).
20. A. Korpel, Acoust. Holog., 2, 39-52, Plenum Press (1970).
21. A. Korpel, Drukkerij Bronder-Offset N.V., Rotterdam (1969).
22. J. Landry, et al., Acoust. Holog. Vol. 3, 47-125, Plenum Press (1971).

23. R. A. Smith, Acoust. Holog., 5, 7-9, Plenum Press (1973).
24. R. Adler, A. Korpel and P. Desmares, IEEE Trans. on Sonics and Ultrasonics SU-15, 157 (July 1968).
25. L. W. Kessler, P. R. Palermo and A. Korpel, Acoust. Holog. 4, 51-72, Plenum Press (1972).
26. R. L. Whitman, M. Ahmed and A. Korpel, Acoust. Holog. 4, 11-32, Plenum Press (1972).
27. B. B. Brenden, Acoust. Holog. 4, 1-9, Plenum Press (1972).
28. A. Korpel, et al., Acoust. Holog. 5, 15-23, Plenum Press (1973).
29. R. Mezrich, D. Vilkomerson and K. Etzold, App. Optics 15, 1499 (June 1976).
30. A. Chutjian and R. J. Collier, J.O.S.A. 57, 1405 (1967).
31. S. Sokolov, U.S. patent #2,164,125.
32. D. Fritzler, E. Marom and R. K. Mueller, Acoust. Holog. 1, 249-256, Plenum Press (1969).
33. A. F. Metherell and H. M. A. El-Sum. App. Phys. Letters 11, 20-22 (July 1, 1967).
34. H. M. A. El-Sum, et al., J. Acoust. Soc. Am. 42 (4), 733-742 (Oct. 1967).
35. H. M. A. El-Sum, Acoust. Holog. 2, 12-16, Plenum Press (1970).
36. A. F. Metherell, S. Spinok and E. J. Pisa, Acoust. Holog. 2, 69-86, Plenum Press (1970).
37. J. L. DuBois, Acoust. Holog. 2, 59-68, Plenum Press (1970).
38. J. E. Jacobs and Donald A. Peterson, Acoust. Holog. 5, 633-645, Plenum Press (1973).
39. J. E. Jacobs, Trans. N. Y. Academy of Sciences, Series II, 30, 3 (Jan. 1968).
40. R. C. Addison, Acoust. Holog. 5, 659-670, Plenum Press (1973).
41. J. E. Jacobs, Acoust. Holog. 6, 661-669, Plenum Press (1974).
42. P. Buchman, Ferroelectrics 5, 39-43 (1973).
43. P. Alais, Acoustic Holog. 4, 237-249, Plenum Press (1972); Acoust. Holog. 5, 671-684, Plenum Press (1973).

44. A. K. Nigam, et al., Acoust. Holog. 4, 173-194, Plenum Press (1972); Acoust. Holog. 5, 685-700, Plenum Press (1973).
45. G. S. Kino, C. DeSilets, J. Fraser and T. Waugh, IEEE Ultrasonic Symposium Proceedings 75 CHO 994-4SU, 94-101 (1975).
46. W. P. Leung, R. A. Mills, H. J. Shaw, D. K. Winslow and L. Zitelli, IEEE Ultrasonic Symposium Proceedings 75 CHO 994-4SU, 84-87 (1975).
47. J. T. Walker and J. D. Meindl, IEEE Ultrasonic Symposium Proceedings 75 CHO 994-4SU, 80-83 (1975).
48. J. Fraser, J. Howlice, G. Kino, W. Leung, H. Shaw, K. Toda, T. Waugh, D. Winslow and L. Zitelli, Acoustical Holog. 6, 275-304 (1974).
49. J. F. Havlice, G. S. Kino, J. S. Kofol and C. F. Quate, Acoust. Holog. 5, 317-333 (1973).
50. N. Takagi, T. Kawashima, T. Ogura and T. Yamada, Acoust. Holog. 4, 215-236 (1972).
51. N. H. Farahat, IEEE Ultrasonic Proc. 75 CHO 994-4SU, 68-72 (1975).
52. S. A. Farnow and B. A. Auld, Appl. Phys. Letters 25, 681 (1975).
53. S. A. Farnow and B. A. Auld, Acoust. Holog. 4, 259-273 (1972).
54. K. Wang, H. Shen and G. Wade, IEEE Proc. 62, 650 (1974).
55. K. Wang, H. Shen and G. Wade, IEEE Ultrasonic Symp. Proc. 75 CHO-4SU, 52-56 (1975).
56. B. A. Auld, private communications.
57. D. Gabor, Ultrasonic Imaging and Holography, 151-158, Plenum Press (1973).
58. Y. Kikuchi, Ultrasonic Imaging and Holography, 245, Plenum Press (1973).
59. J. E. Jacobs, D. W. Cugell and N. V. Phan, International Conf. on Medical Electronics, Proceedings (P. L. Frommer, ed.) 21, (1961).
60. N. V. Phan, M. S. Thesis, "The Application of T.V. Scanning Techniques to the Problem of Visualizing Ultrasound Images", Northwestern University, Evanston, Illinois (1961).
61. Harold Berger, ANL Report #6680.
62. Harold Berger, Acoust. Holog. 1, 30-34 (1969).

63. S. J. Sokolov, Techn. Physics USSR 3, 176-182 (1936).
64. N. Marinesco and J. J. Truillet, Compt. Rend. 196, 858-860 (1933).
65. G. S. Bennett, J. Acoust. Soc. Am. 25, 1149-1151 (1953).
66. H. Berger and I. R. Kraska, J. Acoust. Soc. Am. 34, 518-519 (1962).
67. Y. Torkikai and K. Nigishi, J. Phys. Soc. Japan 10, 1110-1113 (1955).
68. M. E. Arkhangel'skii and V. Ia. Afanas'ev, Soviet Physics-Acoustics 3, 230-235 (1957).
69. G. S. Bennett, J. Acoust. Soc. Am. 24, 470-474 (1952).
70. R. Haul, H. J. Studt and H. H. Rust, Angew. Chemie 62, 186-188 (1950).
71. R. Haul, H. J. Studt and H. H. Rust, Naturwissenschaften 36, 374-375 (1949).
72. H. H. Rust, Angew. Chemie 64, 308-311 (1952).
73. P. Renaud, J. Chim. Phys. 52, 339 (1955).
74. L. D. Rozenberg, Soviet Phys.-Acoustics 1, 105-116 (1955).
75. P. J. Ernst and C. W. Hoffman, J. Acoust. Soc. Am. 24, 207-211 (1952).
76. W. S. Colburn and K. A. Haines, App. Optics 10, 1636-1641 (July 1971).
77. B. L. Booth, App. Optics 14, 593-601 (March 1975).
78. L. W. Kessler and S. T. Sawyer, Appl. Phys. Letters 17, 440-441 (1970).
79. J. F. Havlice, Electronics Letters 7, 477-479 (1969).
80. P. Greguss, Laser and Unconventional Optics Journal #45 (published by European Abstracts Service, Goteborg, Sweden).
81. P. Greguss, Acoustica 29, 52 (1973).
82. J. L. Ferguson, Acoust. Holog. 2, 53, Plenum Press (1970).
83. G. H. Brown, G. J. Dienes, and M. M. Labels, "Liquid Crystals", Gordon and Breach, New York (1966).
84. M. J. Intlekofer, and D. C. Auth, App. Phys. 20, 151-152 (1972).
85. H. Mailer, App. Phys. Letters 18, 105-106 (1971).

86. R. Z. Pohlman, Physik 113, 697 (1939).
87. R. Pohlman, Z. Agnew. Phys. 1, 181 (1948).
88. H. E. Van Valkenburg, Abstract #U8, 74th OAS Meeting (1967).
89. J. D. Young and J. E. Wolfe, App. Phys. Letters 11, 294-296 (1967).
90. W. A. Penn and J. L. Chovan, Acous. Holog. 2, 168-169 (1970).
91. H. M. A. El-Sum, Acoustic Holography 1, 14-22, Plenum Press (1969).
92. B. B. Brenden, Acoustic Holography 1, 65-71, Plenum Press (1969).
93. J. L. Kreuzer, Acoustic Holography 1, 73-95, Plenum Press (1969).
94. K. Preston, Jr. and J. L. Kreuzer, App. Phys. Letters 10, 150-152 (1967).
95. G. E. Massey, Proc. IEEE 55, 1115-1117 (1967).
96. J. W. Goodman, Acoust. Holog. 1, 173-186, Plenum Press (1969).
97. P. Gregus and H. J. Caulfield, Science 177, 422-424 (1972).
98. G. W. Stroke, Wcience 189, 994-995 (1975).
99. H. M. A. El-Sum, Acoust. Holog. 1, 19-22 (1969).
100. A. Korpel and P. Desmares, J. Acoust. Soc. Am. (Sept. 1968).
101. R. Adler, A. Korpel and P. Desmares, paper #3, IEEE Symp. on Sonics and Ultrasonics (Vancouver, Canada, 1967).
102. H. Berger, Acoust. Holog. 1, 34-36 (1969).
103. A. F. Metherel and H. M. A. El-Sum, Proc. Symp. Eng. Uses of Holography, Scotland, Sept. 1968 (Cambridge University Press).
104. H. M. A. El-Sum, Acoustical Holography, 2, 16, Plenum Press (1970).
105. H. M. A. El-Sum, Acoustical Holography, 2, 16-19, Plenum Press (1970).
106. B. P. Hilderbrand and K. A. Hains, Physics Letters 6, 378 (1968); and J.O.S.A. 59, 1 (1969).
107. L. Larmore, H. M. A. El-Sum and A. F. Metherell, App. Opt. 8, (8), 1533-1536 (1969).
108. M. G. Maginess, J. D. Meindl, et al., IEEE Proc. Symposia on Sonics and Ultrasonics (1973 and 1975); Acoust. Holog. 5, 619-631, Plenum Press (1973); Stanford Cardiac Imaging Conference (July 1975).

109. K. R. Erikson, F. J. Fry and J. O. Jones, IEEE Trans. Sonics and Ultrasonics, SU-21 (3), 144-170, (July 1974). (This reference contains 376 references related to Ultrasonics in Medicine.)
110. H. M. A. El-Sum, "Optical Processing of Information", 85-97, Spartan Publishers (1963).

APPENDIX A

EARLIER STUDY OF THE PROJECT

I. INTRODUCTION

1.1 GENERAL REMARKS

The flurry of activity in acoustical imaging of the 1930's and early 1940's, [1,2] mainly in the USSR and Europe, has been revived with more vigour in the 1960's after the demonstrated success of optical holography and the availability of coherent light sources--lasers. The dormant period in the work on acoustical imaging resulted mainly from the difficulties encountered in making satisfactory acoustic lenses on one hand, and on the other hand, from the inability to produce reliable and/or low cost acousto-optical transducers capable of transforming the acoustical image to a visible one.

Holography seems to alleviate these two main difficulties since, in principle, no lenses were needed and the acoustical hologram may be in itself considered as the acousto-optical transducer. [3,4] Since the early publication of the original theory of holography [5] by D. Gabor in Great Britain, and the early work of El-Sum [6,7] in the USA, it was known that the technique of holography can be extended to all scalar waves, including acoustic waves. Demonstration of this was made with electrons, [6,8] x-rays [7] and microwaves [9] in the 1950's; however, acoustic holograms were made about two decades later. [10] The delay was mainly due to the nonavailability of coherent light sources (lasers) and the lack of proper practical techniques for interfacing acoustical and optical fields in order to render an intelligible visible picture of the acoustical image.

In light of the brief discussion mentioned above, we shall survey the various categories of acoustic holography and the interfacing of the

acoustical and optical fields as applied in particular to nondestructive testing. For a coherent discussion we shall describe first, very briefly, the general theory of holography.

1.2 SIMPLIFIED THEORY OF HOLOGRAPHY IN GENERAL

The theory of holography is very well known^[5,6,12,13]. When two coherent waves \vec{U}_0 and \vec{U}_r interfere, the recorded interference pattern registers the intensity I of the resulting wave \vec{U} where

$$\begin{aligned}\vec{U} &= \vec{U}_r + \vec{U}_0 \\ I = \vec{U}\vec{U}^* &= \vec{U}_r\vec{U}_r^* + \vec{U}_0\vec{U}_0^* + \vec{U}_r\vec{U}_0^* + \vec{U}_r^*\vec{U}_0\end{aligned}\quad (1)$$

where the asterisk denotes the complex conjugate.

The first two terms in the above equation (1) represent the intensities of the waves \vec{U}_r and \vec{U}_0 , respectively, while the last two terms represent additional intensities due to the interference between \vec{U}_r and \vec{U}_0 . The recorded pattern is the hologram. The two waves \vec{U}_r and \vec{U}_0 may be considered as a reference wave and an object wave (wave scattered by the object). Assuming linear recording of the intensity I and a linear response of the hologram, it is easy to prove that illuminating the hologram with one of the waves (for example \vec{U}_r) reconstructs the other wave \vec{U}_0 and its complex conjugate \vec{U}_0^* . In other words a replica of the original object is reconstructed together with its complex conjugate or a twin image. The two images can be separated and viewed.

The reconstructing wave need not be of the same wavelength as that used to make the hologram. In other words, \vec{U}_0 and \vec{U}_r may be acoustic waves, while the reconstructing wave is a visible light wave. Thus we have an acoustical hologram reconstructed with visible light.

The dimensions of the reconstructed image, however, will be different from the original object unless the dimensions of the hologram is properly changed before the reconstruction.^[3] When the hologram dimensions are unchanged, the lateral dimensions (x,y) of the object are unchanged, while the depth (z) is distorted in proportion to the wavelength ratio λ_S/λ_L where λ_S is the acoustic wavelength and λ_L is the light wavelength.

If, on the other hand, the scale of the acoustic hologram is reduced by a factor m, the lateral dimensions of the reconstructed image will be reduced by the same factor, while the reduction in depth is proportional to m^2 ; the net scale transformation x' , y' and z' of the reconstructed image will then read

$$\begin{aligned} x' &= mx \\ y' &= my \\ z' &= m^2 (\lambda_S/\lambda_L) z \end{aligned} \tag{2}$$

which shows that to obtain an undistorted image, one must choose $m = \lambda_L / \lambda_S$ which is of the order of 10^{-3} . The image would therefore be so small as to require optical magnification--which would in turn regenerate the depth distortion.

The question next is how does the acoustical hologram be recorded permanently (such as on photographic films for later reconstruction) or temporarily on an appropriate medium (for real time reconstruction).

Table I^[14] lists the various classes of ultrasonic detectors (frequency > 20 ^k MHz).

The choice of a particular technique for recording an acoustical hologram depends upon the frequency of the interaction of the sound with

the subject under study. As a guide for the choice of the appropriate sonic frequency for various applications, Table II may be used as a guide.^[15] For nondestructive testing, frequencies in the range of 100 KHz to 10 MHz are used for detection of macroscopic flows. The techniques of mapping the acoustic field into an optical one vary according to the acoustic frequency used. Furthermore, the coupling between the tested object and the medium of acoustic wave propagation depends, also, on the acoustic frequency. We shall emphasize in this proposal techniques applicable to nondestructive testing of macroscopic, nonbiological objects.

Table I. Ultrasonic Detectors (Frequency > 20 KHz)

<u>Class of Detector</u>	<u>Minimum Detect Power (watt/cm)</u>
Photographic and Chemical (direct effect on particularly soft emulsion; change in resistance of emulsion to fixing; change in developing speed; oxidizing reaction.)	1
Thermal (thermocouples; thermistors; thermopiles; semiconductors; photoemitters; organic materials which change color, such as iodine, chlorine, chromotropics; liquid crystals; stimulators or extinguishers of luminescence; phosphor persistence devices)	0.1
Optical and Mechanical (Schlieren method; use of birefringence due to stress; surface deformation of solids or fluids; suspended aluminum flakes)	10^{-4}
Electronic (piezoelectric effect; electrostrictive; piezoresistive; piezoelectric plus electroluminescence)	10^{-11}

Table II. Frequency Range for Different Applications

<u>Applications</u>	<u>Frequency Range of Sound</u>
Geophysics	~ 100 Hz for deep penetration 100 to 10,000 Hz for oil, mineral prospecting and archaeology
Oceanography	5 to 100 KHz for long to short range 3-D imaging under water
Nondestructive Testing and Medical Diagnosis	100 KHz to 10 MHz
Ultrasonic Microscopy	10 MHz to 10 GHz

II. METHODS AND TECHNIQUES OF ACOUSTO-OPTICAL HOLOGRAPHY AND ACOUSTO-OPTICAL INTERFACING

Acoustical imaging and acousto-optical interfacing (coupling) are interdependent and will be dealt with as such in this section.

There are many ways of categorizing the methods and techniques of acoustical holography. [3,4,15,16,17] Such methods fall in one or a combination of the following classes:

- Surface deformation (liquid and solid)
- Scanning (mechanical, electronic and laser beam)
- Direct light - sound interaction (Bragg diffraction)
- Direct conversion for instantaneous display (liquid crystals)

The following are brief discussions of some of these methods, presented merely to illustrate the general idea of the techniques.

2.1 LIQUID SURFACE DEFORMATION WITH ACOUSTIC REFERENCE WAVE.

When two acoustic beams (object and reference beams) propagate in a liquid medium, their interference affects the free surface of the liquid, according to the pressure equilibrium equation:

$$\rho gh - \gamma \nabla^2 h = 2P \quad (3)$$

where P , ρ , γ and h are the acoustic pressure, the density of the liquid, its surface tension, and the surface deformation, respectively. The whole liquid surface is levitated by h_0 , while the ripples (height h) are spaced a distant d apart, which, from Eq. (3) will be:

$$\left. \begin{aligned}
 h &= \frac{I \cdot C}{2\pi^2 \gamma f_S^2 \sin^2 \theta_S} \\
 d &= \frac{\lambda_S}{2 \sin \theta_S} \\
 h_o &= \frac{4I}{g\rho C}
 \end{aligned} \right\} \quad (4)$$

where I is the sound intensity, C and f_S its velocity and frequency, θ_S half the angle between the reference and object beam.

The rippled surface can be considered as a phase hologram which may be reconstructed optically by illuminating it with a coherent light beam, incident on the surface at an angle θ_L such that

$$\frac{\sin \theta_L}{\lambda_L} = \frac{\sin \theta_S}{\lambda_S} \quad (5)$$

Unless the general levitation, h_o , of the surface is uniform or spherical, such levitation produces undesirable noise which should be minimized by choosing the proper parameters of the liquid [Eq. (4)]. On the other hand, h should be maximized in order to have the highest optical diffraction efficiency. Branden and Smith^[18] recommended that as a compromise, a good working criterion is

$$f_S (\text{MHz}) \sin \theta_S \cong 0.233 \quad (6)$$

Other sources of noise in this technique may also be minimized by using an in-focus or image hologram instead of the lensless holography by focusing the insonified object onto the liquid surface (using proper acoustic lenses). The reference beam is directed to the surface to form

the image hologram. Such technique has advantages and disadvantages, in addition to several limitations which will be dealt with in the course of the study.

2.2 LIQUID SURFACE DEFORMATION WITHOUT ACOUSTIC REFERENCE WAVE (Time-Independent Spatial Carrier Imaging)

Instead of a reference beam, Green^[19] used a wire grating close to the surface on which the acoustic image of the object, immersed in the liquid, is projected. In this way, the undesired high frequency ripples, superimposed on the main ripples of the surface and which is unavoidable in Brenden-Smith arrangement, ^{are} is reduced considerably. The optical intensity at the image plane of Green's arrangement is proportional to the square of the acoustic intensity transmitted through the object, and hence is higher than Smith-Brenden arrangement. However, this is not a too important advantage, since it can be compensated for by appropriately choosing the response characteristic of the optical detector. In general the two techniques produce images of comparable quality.

2.3 LIQUID SURFACE DEFORMATION WITH SIMULTANEOUS SCANNING OF THE ACOUSTIC SOURCE AND LIGHT DETECTOR (Synthetic Aperture)

To avoid the distortion of the reconstructed image, brought about by the extreme difference between the acoustic and light wavelengths, El-Sum^[19] and Hilderbrand, et al.,^[20] used a synthetic aperture technique. In this scheme both the detector and the source are scanning with either different or the same velocities. The resultant is a hologram with an equivalent larger aperture and consequently less distortion in the reconstructed image, higher resolution and less speckle noise.

The best results for improvement are obtained when the source and the detector are superimposed and move with the same velocity. Another method to reduce the speckle noise has been proposed by Gabor^[21] and is described next.

2.4 DYNAMIC SURFACE DEFORMATION

When sound passes through a transparent thin film in an acoustic medium, no radiation pressure develops, but the film, nevertheless, moves with the sound. The excursion Δ is given by:

$$\Delta \propto \frac{\sqrt{I_S}}{f_S} \quad (7)$$

I_S and f_S being the acoustic intensity and frequency, respectively. If the film is chosen to be reflective to light, the acoustic excitation passing through the film can be picked up as phase modulation on a coherent light beam. This is the main idea of Gabor^[21]. A single short pulse is sent as a thin film into the body to be investigated. Light reflected from the film produces a Fresnel hologram. Its volume is limited to a very thin layer and hence the omnipresent speckle noise is eliminated from the system.

2.5 INSTANTANEOUS HOLOGRAMS

A record of the instantaneous value of a dynamically deformed surface is equivalent to the information-carrying part of an on-axis hologram. Consecutive recording of two pulsed optical holograms spaced in time by an odd number of acoustic half-waves, and provided that the optical references of the two holograms differ by $\pi/2$, the reconstruction of such a composite hologram gives a phase-contrast image of the acoustic

image over the excited surface.^[22] This in turn can be used as an acoustic hologram.

2.6 RAPID LASER BEAM SCANNING

A laser beam scanned over a reflecting surface picks up the local acoustic excitation as phase modulation. Korpel, et al.^[23] demonstrated the idea using a lens to image the exit pupil of the beam deflector onto the entrance pupil of the detector. A knife edge in front of the photodiode detector transforms the phase modulation of the beam into amplitude modulation, producing a signal proportional to the acoustic excitation. The signal is then processed and displayed on a CR tube from which a record can be made for optical reconstruction. This scheme, however, is limited in resolution and in aperture, and hence is usually limited to ultrasonic microscopy.

2.7 ELECTRON BEAM SCANNING OF ACOUSTICALLY DEFORMED SURFACE

A less sensitive scheme than the laser scanning one is to image the acoustically deformed surface onto a photocathode. The electron image is then scanned electrically. This scheme is capable of displaying either a hologram or its optical reconstruction, depending on the location of the photocathode in the optical system.^[24]

2.8 PIEZOELECTRIC TRANSDUCERS

Many materials (quartz, lithium sulfate, barium titanate, lead zirconate-titanate, lead metaniobate, etc.) are used as either transducers or detectors. For imaging, the transducer (or the object) is scanned mechanically,^[25] or by making use of an array of transducers.

Since a piezoelectric transducer acts as a mosaic (transducers array), the acoustic wave incident on it produces an equivalent electric

image across it. The transducer surface can then be scanned by an electron beam in order to generate a television-type signal. Acoustic television camera, based on this principle, was first made by Sokolov.^[26] Barium titanate or quartz has been used in such cameras. They have a good dynamic range (3×10^{-9} to 3×10^{-3} W/cm²) and a low sensitivity threshold of 2×10^{-11} W/cm². However, they have a limited aperture and a narrow angular field of view. Such tubes have been used to record and reconstruct acoustic holograms^[27] with real or simulated reference wave.^[35]

2.9 PIEZORESISTIVE DETECTORS^[28]

A CdS(Cu) has high electric resistivity and its conductivity changes with an incident acoustic wave. A vidicon-type camera tube using such a target has mainly three advantages over the piezoelectric type tube:

- (a) It responds to a wide range of acoustic frequencies as opposed to the resonant frequency and odd harmonic response of the piezoelectric type.
- (b) It has the capability of information storage.
- (c) It has higher sensitivity.

2.10 ELECTROLUMINESCENT DETECTOR

This is mainly a piezoelectric material with an electroluminescent coating having a proper thickness and, additionally, simulated for luminescence with either a bias voltage or ultraviolet illumination. Such a detector has a sensitivity of 10^{-6} - 10^{-7} W/cm². Voltages generated by the acoustic wave incident on the piezoelectric side, appear at the interface with the electroluminescent layer.

2.11 POHLMAN CELL [29]

A cell filled with xylene in which small aluminum flakes are suspended is used for acoustic image detection. In the presence of acoustic wave incident on the cell, the Al flakes are aligned and they reflect light incident on the cell. With no acoustic wave present, the flakes are randomly oriented and present a grey background by the reflected light; this background can be eliminated, in order to produce a better contrasting image, by applying a small bias voltage across the cell.

2.12 LIQUID-CRYSTAL ACOUSTICAL-TO-OPTICAL CONVERSION CELL [30,31]

A thin layer of nematic liquid crystals sandwiched between a polarizer and a glass plate treated in such a way that the liquid crystals float freely in their low-energy state, and hence are aligned on one axis only. Since the liquid crystals are birefringent, they act as a wave plate, and when an acoustic wave is projected on such a liquid-crystal cell, the directions of the molecules change, causing a change in the optical transmission pattern. Thus the acoustic wave information is transformed into visible information. The sensitivity of such cells is demonstrated to be of the order of a few mW/cm^2 , and the aperture attained so far is not too large (~ 25 cm square). The image resolution attained is reasonable and shows the fringes of an acoustical hologram made with 3 MHz wave.

2.13 BRAGG DIFFRACTION

This is a direct interaction of light and sound, capable of real time visualization of acoustic images. [32] A visible image of the insonified object is formed when the angle θ between the acoustic waves and the

direction of propagation of a coherent light beam satisfies Bragg's condition

$$2\lambda_S \sin \theta = \lambda_L \quad (8)$$

where λ_L is the wavelength of the light inside the medium and λ_S is the acoustic wavelength. This necessitates an almost perpendicular illumination of the acoustic field. The image formed is usually demagnified by the ratio of λ_L/λ_S , and its resolution depends on the size of the light source. Such images are usually of low intensity.

The maximum usable acoustical frequency in this technique is 20-30 GHz and it is usually limited to microscopic objects.

2.14 BIREFRINGENT CRYSTALS IN ACOUSTICAL MICROSCOPY^[33]

LiNbO_3 birefringent crystals are used as the acoustic propagating medium.^[34] The light propagates coaxially in the crystal in an opposite direction to the acoustic wave. From the conservation of energy and momentum of the interacting fields, one finds that

$$(\lambda_S)_{\max} = \frac{\lambda_L}{n_E - n_O} \quad (9)$$

where n_E and n_O are indices of refraction of the extraordinary and ordinary waves in the crystal. This yields minimum acoustic frequency limit, and hence allows an extremely high frequency to be used in microscopic objects visualization.

This technique, however, is limited to microscopic objects.

2.15 MISCELLANEOUS OTHER TECHNIQUES

Meindl, Walker and Maginess^[36] developed a new acoustic camera for real time visualization of insonified optics. Such a camera uses

integrated electronic circuits, acoustic lenses, and electron beam scanning of detector arrays. Although the technique is not based on the theory of holography, its exploration by itself and its possible application to holography is worth consideration.

Microwave acoustics is also gaining keen interest by many workers in the field of acoustical imaging. One approach is the use of electronic scanning of a focussed acoustic beam, where the focussing and steering of the acoustic waves are produced by means of inhomogeneity and anisotropy induced by applied magnetic and electric fields. A collimated acoustic beam has been scanned over an angle of 8° in a uniform magnetic field, and a 125- μ -diameter acoustic beam has been produced by focussing in a nonuniform field. [37]

Various developments and refinements in acoustical imaging techniques has been reported recently in the 1975 Ultrasonic Symposium. [38]

Further information on coherent optical processing of acoustical information can be found in reference 39.

REFERENCES

1. Berger, H., Acoustical Holography, vol. I, Metherell, El-Sum, et al. (Plenum Press, 1969) pp. 27-48.
2. Berger, H., and Dickens, R. E., Report ANL-6680 (1963).
3. El-Sum, H. M. A., ref. 1, pp. 1-26.
4. El-Sum, H. M. A., Acoustical Holography, vol. II (Plenum Press, 1970) pp. 7-22.
5. Gabor, D., Nature 161, 777 (1948); Proc. Roy. Soc. 197A, 454 (1949); Proc. Roy. Soc. 64B, 449 (1951).
6. El-Sum, H. M. A., Ph.D. Thesis (Stanford University, 1952).
7. Kirkpatrick, P., and El-Sum, H. M. A., J.O.S.A. 46, 825-831 (1956).
8. Haine, M. E., and Mulvey, T., J.O.S.A. 42, 763 (1952).
9. Patty, et al., Proceedings National Electronics Conference 10, 1-13 (February, 1955); U.S. NOL, A Report, #6228 (January, 1959).
10. Mueller, R. K., and Sheridan, N. K., App. Phys. Letters 9, 328 (1966).
11. Acoustic Holography, vol. I (Plenum Press, 1969).
12. Optical Holography by R. J. Collier, et al. (Academic Press, 1971).
13. Goodman, J. W., Proc. IEEE 59, 1292 (1971).
14. El-Sum, H. M. A., Holography Seminar Proceedings (SPIE, 1968).
15. Mueller, R. K., Proc. IEEE 59, 1319 (1971).
16. Greguss, P., Phys. Today 27, 42 (1974).
17. Wade, J., private communications and paper to be published.
18. Smith, R. B., and Brenden, B. B., IEEE Symposium on Sonics and Ultrasonics, N.Y., (Sept., 1968).
19. El-Sum, H. M. A., ref. 4, pp. 16.
20. Hilderbrand, R. P., and Haines, K. A., Phys. Letters 6, 378 (1968); J.O.S.A., 59, 1 (1969).
21. Gabor, D., U.S. Patents Nos. 548939 and 3745814 (1973).
22. Metherell, et al., Ref. 4, pp. 394.

23. Korpel, A., and Desmaris, P., J. Acoust. Soc. Am. 45, 881 (1969).
24. Chutjian, A., and Collier, R. J., J.O.S.A. 57, 1405 (1967).
25. Martin, G., Brit. J. NDT 9, 27 (1967).
26. Sokolov, S., U.S. Patent 2,164,125.
27. Fritzler, D., et al., Acoustic Holography, vol. I (Plenum Press, 1969), pp. 249.
28. Jacobs, J. C., U.S. Patent 3,236,944.
29. Pohlman, R, Z. Physik 113, 697 (1939).
30. Greguss, P., Acoustica 29, 52 (1973).
31. Ferguson, J. L., Acoust. Holography, vol. II (Academic Press, 1970), pp. 53.
32. Korpel, A., Appl. Phys. Letters 9, 425 (1966).
33. Quate, C., and Havlice, J., Stanford University, private communications; Havlice, J., Quate, C. F., and Richardson, B., IEEE Trans. SU-15, 68 (1968); Massey, G. A., Proc. IEEE 56, 2157 (1968).
34. Dixon, R. W., Quantum Electron, QE-3, 85 (1967).
35. Ref. 4, pp. 12.
36. Private discussions. Also, Acoustical Holography, vol. V (Plenum Press, 1973).
37. Auld, B. A., et al., Ref. 4, pp. 117; Acoustic Fields and Waves in Solids, vols. I and II (Wiley Interscience, 1973).
38. IEEE Proceedings of the 1975 Ultrasonic Symposium (under publication).
39. El-Sum, H. M. A., AGARD Conference Proceedings 50 (1970).

APPENDIX B

REAL-TIME, ERASABLE IMAGE RECORDING

The electronically focussed, electronically scanned piezoelectric mosaic array used for acoustical imaging plays the role of the photographic films in detecting optical images. It is fast and sensitive.

Another group of recording devices is the Ruticon^(B-1) family. Such devices are based on surface deformation using photoconductors like the thermoplastic sandwiches^(B-2,3), the photomembrane light modulator^(B-4) and the Elmikon^(B-5). Surface-deformation imaging was first proposed for electron-beam addressing of deformable liquid or elastomer surfaces in the Eidophor systems^(B-6), in light valves^(B-2,7,8), and in the deformatographic storage and display tube^(B-9,10).

The "Ruticon" temporarily store an input image as a surface-deformation pattern on an elastomer layer. It is a layered structure consisting of a transparent conductive substrate, as shown in Fig. B-1, a photoconductor layer (usually poly-N-vinyl-carbazole with a green organic sensitizér dye and an elastomer layer, usually of the siloxane-based variety). When the photoconductor is exposed to image light, the voltage distribution across the photoconductor changes, in turn causing changes in the electric field across the elastomer layer. The resulting distribution of electromechanical forces across the elastomer causes it to deform into a surface relief pattern corresponding to the image light. This deformation persists after the optical image has been removed, as long as the field is maintained. Ruticons are suitable for recording holograms and continuous-tone incoherent images at exposure levels of less than 300 erg cm^2 ($3 \times 10^{-5} \text{ W/cm}^2$ for 1 sec exposure, $5 \times 10^{-7} \text{ W/cm}^2$ for 1 min exposure, or 3×10^{-4} for 0.1 sec. exposure), with a resolution in excess of 850 line pairs/mm. The "Ruticons" are read out with a

phase-sensitive optical system (Schlieren) as shown in Figure B-2. It can be used for incoherent-to-coherent image conversion, spatial filtering, correlation, wavelength conversion, image intensification, buffer storage of optical information, and real-time display (since they can be erased to less than 10 percent of their initial intensities within 10 msec.

Although the use of dielectric liquid (with or without applied electric field) was demonstrated as a promising deformable surface to detect acoustical holograms and images, the Ruticon has never been tested for acoustical imaging. However, its optical behavior may prove useful for the hybrid system of nondestructive testing (Figure 1).

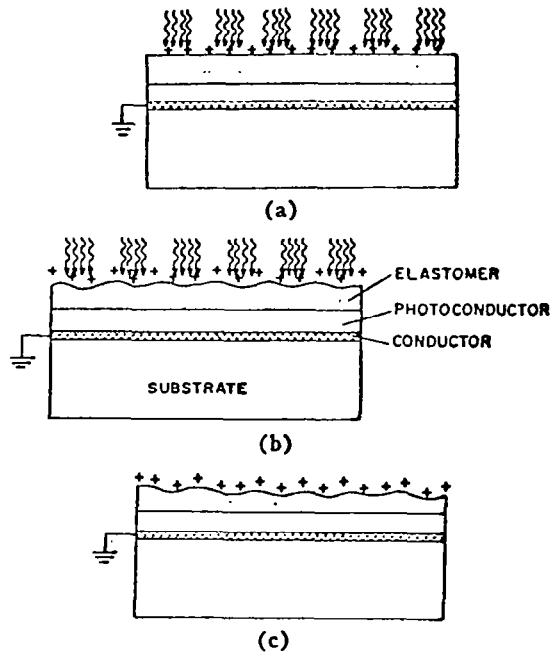


Figure B-1. Operation of Ruticon imaging devices. First, a charge is placed on the elastomer surface (a) by means of corona discharge, glow discharge, contact with a liquid metal, or a thin flexible metal layer deposited on the surface of the elastomer. Then, the photoconductor is exposed to image light (e.g. a bar pattern is used in this illustration). The elastomer surface deforms into a relief pattern corresponding to the optical image, as seen in (b). After the removal of the optical image, (c), the surface-deformation pattern persists. (After N.K.Sheridan, Ref. B-1)

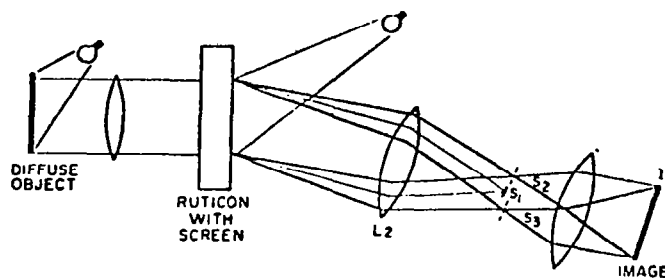


Figure B-2. An arrangement for reading out a Ruticon, used to record and project incoherent images. Opaque stop S_1 prevents the direct light from reaching the output image plane I_2 . By placing stops S_2 & S_3 in the back focal plane of lens L_2 (in place of S_1) a negative image of the input is obtained. When glow-discharge or corona-discharge are used (before recording on the Ruticon) the Ruticon can be viewed by transmission, while images formed by the liquid-metal or metal-plated devices must be read out by reflection (as this Figure illustrates) because of the opacity of the deformable metal electrode.
(After N.K.Sheridon, Ref. B-1)

REFERENCES

- B-1 N. K. Sheridan, IEEE Trans. on Electron Devices ED-19 (9), 1003-1010 (1972).
- B-2 W. Glenn, J. App. Phys. 30 (12), 1870 (1959); J.O.S.A. 48, 841 (1958).
- B-3 R. W. Gundlach and C. Claus, Photo. Sci. Eng. 17, 14 (1963).
- B-4 F. Reizman, AGARD Conf. Proc. 50 (Sept. 1959).
- B-5 W. Baumgartner, Z. Angew. Math. Phys. 18, 31 (1967).
- B-6 F. Fisher and H. Thiemann, Schweiz. Arch. 7, 1, 33, 305, 337 (1941); 8, 15, 1351, 1691, 199 (1942).
- B-7 W. Good, Proc. Nat. Electron. Conf. 24 (1968).
- B-8 E. Bauman, J. Soc. Motion Pict. Telev. Eng. 60, 351 (1953).
- B-9 R. J. Wohl, F. A. Hawn and H. C. Medley, U.S. Pat. 3,626,084 (1971).
- B-10 J. A. van Raalte, J.O.S.A. 9 (10), 2225 (1970).